AD_____

Award Number: W81XWH-08-2-0207

TITLE: Measuring Intracranial Pressure and Correlation with Severity of Blast Traumatic Brain Injury

PRINCIPAL INVESTIGATOR: Dr. Pamela VandeVord

CONTRACTING ORGANIZATION: Metropolitan Detroit Research and Education Foundation
Detroit, MI 48201

REPORT DATE: October 2011

TYPE OF REPORT: Annual

PREPARED FOR: U.S. Army Medical Research and Materiel Command
Fort Detrick, Maryland 21702-5012

REPORT DOCUMENTATION PAGE

Form Approved
OMB No. 0704-0188

1. REPORT DATE *(DD-MM-YYYY)*	2. REPORT TYPE	3. DATES COVERED *(From - To)*
01-10-2011	Annual	16 SEP 2010 - 15 SEP 2011

4. TITLE AND SUBTITLE

Measuring Intracranial Pressure and Correlation with Severity of Blast Traumatic Brain Injury

5a. CONTRACT NUMBER

5b. GRANT NUMBER
W81XWH-08-2-0207

5c. PROGRAM ELEMENT NUMBER

6. AUTHOR(S)
Dr. Pamela VandeVord

E-Mail: pvord@wayne.edu

5d. PROJECT NUMBER

5e. TASK NUMBER

5f. WORK UNIT NUMBER

7. PERFORMING ORGANIZATION NAME(S) AND ADDRESS(ES)
Metropolitan Detroit Research and Education Foundation
Detroit, MI 48201

8. PERFORMING ORGANIZATION REPORT NUMBER

9. SPONSORING / MONITORING AGENCY NAME(S) AND ADDRESS(ES)
U.S. Army Medical Research and Materiel Command
Fort Detrick, Maryland 21702-5012

10. SPONSOR/MONITOR'S ACRONYM(S)

11. SPONSOR/MONITOR'S REPORT NUMBER(S)

12. DISTRIBUTION / AVAILABILITY STATEMENT
Approved for Public Release; Distribution Unlimited

13. SUPPLEMENTARY NOTES

14. ABSTRACT

A greater understanding of the mechanism(s) of TBI due from overpressure exposure is critical to develop effective protection and treatments. Fundamental, yet unresolved, questions concern the mode of blast energy transfer to the brain as well as the consequent damage or disruptive mechanisms at the cellular level. The ultimate goal of this research effort is to determine the intracranial pressure (ICP) responses to blast exposure. The objective of this research is to understand how pressure is transmitted through the brain and ascertain the relationship between levels of pressure transmission with severity of brain injury. Several biomechanical parameters were investigated during this year of the proposal. We used a shock tube model in which instrumented animals were be subjected to a series of systematic shocktube studies of blast-stress transmission to the brain. We demonstrated by this series of tests that the brain-skull system is very sensitive to instrumentation location. Furthermore, we documented that the skull undergoes strain and deformation when exposed to the transient shock wave. Overall, the data key to determining the mechanism of blast energy transmission to the brain.

15. SUBJECT TERMS
Blast, Overpressure, Traumatic Brain Injury, Animal Models

16. SECURITY CLASSIFICATION OF:			17. LIMITATION OF ABSTRACT	18. NUMBER OF PAGES	19a. NAME OF RESPONSIBLE PERSON
a. REPORT	b. ABSTRACT	c. THIS PAGE			USAMRMC
U	U	U	UU	35	19b. TELEPHONE NUMBER *(include area code)*

Table of Contents

Page

Introduction…….. 02

Body…….. 02

Key Research Accomplishments…….. 20

Reportable Outcomes……. 20

Conclusion…… 21

References…… 22

Appendices…… 23

INTRODUCTION

A greater understanding of the mechanism(s) of TBI due from overpressure exposure is critical to develop effective protection and treatments. Fundamental, yet unresolved, questions concern the mode of blast energy transfer to the brain as well as the consequent damage or disruptive mechanisms at the cellular level. The ultimate goal of this research effort is to determine the intracranial pressure (ICP) responses to blast exposure. The objective of this research is to understand how pressure is transmitted through the brain and ascertain the relationship between levels of pressure transmission with severity of brain injury. The aims of this proposal are to (1) map the transient ICP pressure as a function of blast magnitude (2) map the transient ICP as a function of head orientation and (3) ascertain injury severity as a function of ICP. We will use an *in vivo* model in which animals will be subjected to a series of systematic shock-tube studies of blast-stress transmission to the brain. The proposed research is *significant* because resolution of the mode of energy transfer and the induced stress states within the brain will allow for evaluations of mitigation/protective techniques, as well as design of experiments investigating live-cell response.

BODY

Since the last progress report from October 2010, we have undergone several key experiments in order to accomplish our goals. Using the testing system we optimized in the first year of the award, we continue investigating how head orientation effects the animal's ICP measurements. We further identifying key biomechanical parameters that may contribute to the injury occurring form blast. During our testing we have also discovered some challenges with respect to the model. A detailed description of our methodology, results and challenges are presented below.

1.0 Wayne State University (WSU) shock wave generator.

To simulate a free field blast wave in the laboratory, it is convenient to utilize a shock tube activated by compressed gas. In this study the simulated blast waves were generated by a Helium-driven shock tube located at the Wayne State University Bioengineering Center. A shock tube consists of two separate chambers: the driver, where the pressured air is created by means of an air compressor system, and the driven, where the shock wave propagates (Celander 1954). In the simplest shock tube operation, the driver is separated from the driven by a replaceable membrane. For any given material the membrane ruptures at a particular pressure that is directly proportional to its thickness and allows the generation of the shock wave into the driven. Note that because the wave is produced by compressed gas bursting a membrane instead of an actual chemical explosion, we use the term shock wave instead of blast wave. The test section usually contains air at atmospheric pressure before the bursting of the diaphragm. If the diaphragm bursts ideally, a uniform shock front quickly develops and propagates down the test section. If

the cross section of the shock tube is constant, the shock wave moves at constant speed unattenuated down the tube until the reflected rarefaction from the closed end of the driver overtakes it. Prior to this overtaking, the shock waveform will feature a flat section after the peak. Following the overtaking, the waveform for static pressure will have a decaying profile similar to a blast wave. Furthermore, in this regime the dynamic pressure component of the shock wave flow is credibly similar to that of free field blast. However, it is very important to note that this zone within the shock tube appropriate for blast simulation will eventually be affected by the arrival of disturbances and gas dynamic features entirely atypical of blast waves. Example of such anomalous disturbances might be the arrival of the contact surface with expanding driver gas, or the arrival of the strong rarefaction from the open end of the tube. At some locations within the tube, the effects of these anomalous flow features are exaggerated and will corrupt the experimental conditions much earlier. Extremely adverse effects will result from experiments staged with a specimen near the end of the tube where the end-rarefaction will quickly cause imbalance of high dynamic pressures yet reduced static pressure conditions. The specimen in this regime would in fact be subjected to a nearly pure jet-stream outflow, exaggerated under-pressures or vacuum, or indeed a shock propagating upstream. ***Thus, our testing methods always place the animals 44 inches up from the end of the shock tube.***

1. EVALUATING THE ICP EFFECT FROM INSTRUMENTATION LOCATION

The results from our previous experiments demonstrated that the rat skull is very thin and the addition of instrumentation to the top of the skull could potentially be influencing the data. The mounting of the fiber optic pressure sensor on the superior skull case may change the frequency response of the skull under shock wave loading. To address this concern a series of tests were developed to determine if mounting of the fiber optic pressure sensor on the occipital bone would report unique ICP profiles. Additionally, to investigate the effect of skull maturation on pressure recordings, older rats were included in this study to determine if age affects the ICP response. Approval from the Wayne State University Animal Investigation Committee was obtained prior to testing.

Two different groups of rats were designated for this study. Group 1 consisted of male Sprague Dawley rats (N=12) that were instrumented with a cannula mounted to the superior aspect of skull (IC). Group 2 consisted of male Sprague Dawley rats (N=6) that were instrumented with a cannula mounted through the occipital bone (OIC).

The superior mounted test set-up (IC) was similar to the methodology described prior and is demonstrated in Figure 1A. The installation procedure for the rats with the occipital mount (OIC) differed from the IC. In brief, rats were euthanized with an overdose of ketamine/xylazine. The scalp of the posterior region was removed. A small hole was then drilled into the bone to allow for the cannula to be placed. Screws were then drilled into the bone at four positions on the occipital bone to be used as anchor points. The cannula with its threaded cap was placed and bone cement was applied to hold the cannula system. Following curing of the cement (~ 10

minutes) the ICP sensor was then sealed within the cannula, with the sensor tip exposed beneath the region between the lambda and bregma (Figure 1B).

d

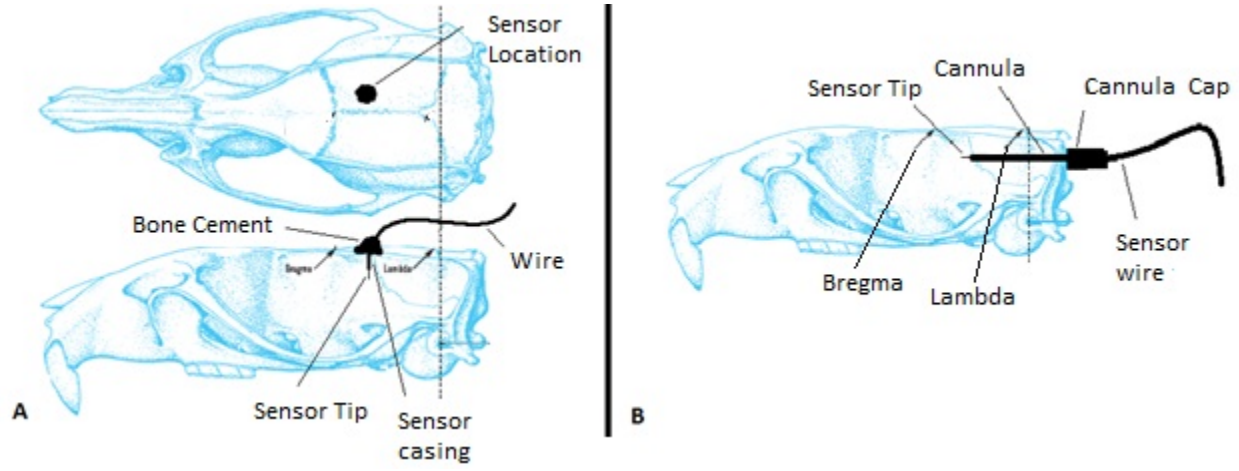

Figure 1. A schematic of the mounting procedures for the IC (A) and OIC (B) mounting positions of the rat skull. Drawings are not to scale.

After instrumentation, rats are placed in the holder positioned the rat's head at 44 inches from the open end of the tube, facing the shock wave frontally. By means of a long rod, the holder was connected to a trolley positioned outside the tube. The purpose of this moveable cart is to minimize stresses imparted to the specimen due to its restraint in the shock wave flow (Figure 2).

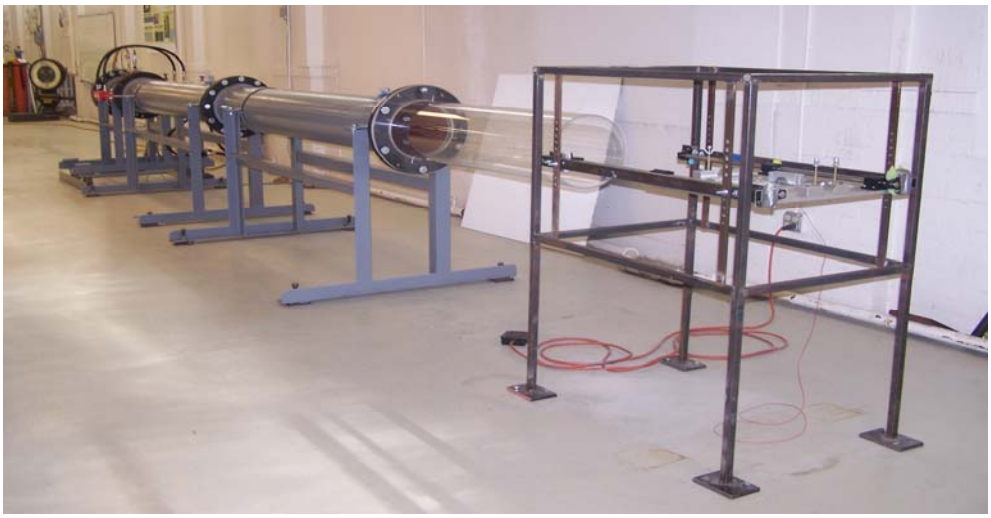

Figure 2. WSU Bioengineering Center Shock Tube.

1.2. Methods for comparing top mounted and back mounted pressure sensors

Each rat was exposed to three shock wave exposures at a given intensity. The intensities ranged from 69 to 172 kPa peak static pressure shock wave intensities. The time in between each exposure was approximately two minutes. Following testing, rats from the IC group were euthanized. The purpose for euthanizing the OIC group prior to testing was undertaken due to the severity of the surgical technique. A table describing the characteristics of the rats tested in the study is provided in Table 1.

Table 1. A description of the weight and mount type for each rat used in the study.

Mount	Weight	Mount	Weight
Top	239	Occipital	264
Top	240	Occipital	232
Top	244	Occipital	238
Top	249	Occipital	290
Top	256	Occipital	317
Top	259	Occipital	325
Top	273		
Top	301		
Top	368		
Top	369		
Top	437		

Pressure data were collected at 400 kHz by the DASH HF. The peak ambient pressure and peak ICP magnitudes were recorded. The peak ICP pressures were grouped by incident intensity and compared with ANOVA. This was also completed for the ratio of peak ICP/peak ambient, where following ANOVA, the *post hoc* Tukey HSD test was conducted to determine significance amongst each group.

For each rat, a unique frequency waveform was observed where first five cycles were counted for the response where the waveform oscillated the most harmonically. Approximate frequencies were then calculated from these cycles using simple wave form analysis. The relationships between weight of the rat, shock wave intensity, and calculated frequency were then described graphically using the contour map method where weight of the specimen and shock wave intensity were graphed on the x and y axes and "contour" of the frequency response was then created using DPLOT (Hydesoft Computing LLC).

1.3. Results for top mounted versus back mounted sensors

For the IC mount, the intracranial pressure response for a 256 gram and a 437 gram rat is shown below in Figure 3. Two major waveforms were observed in the overall pressure profile; (1) secondary high frequency wave form following compression and (2) a large transient response that mirrors the external pressure wave.

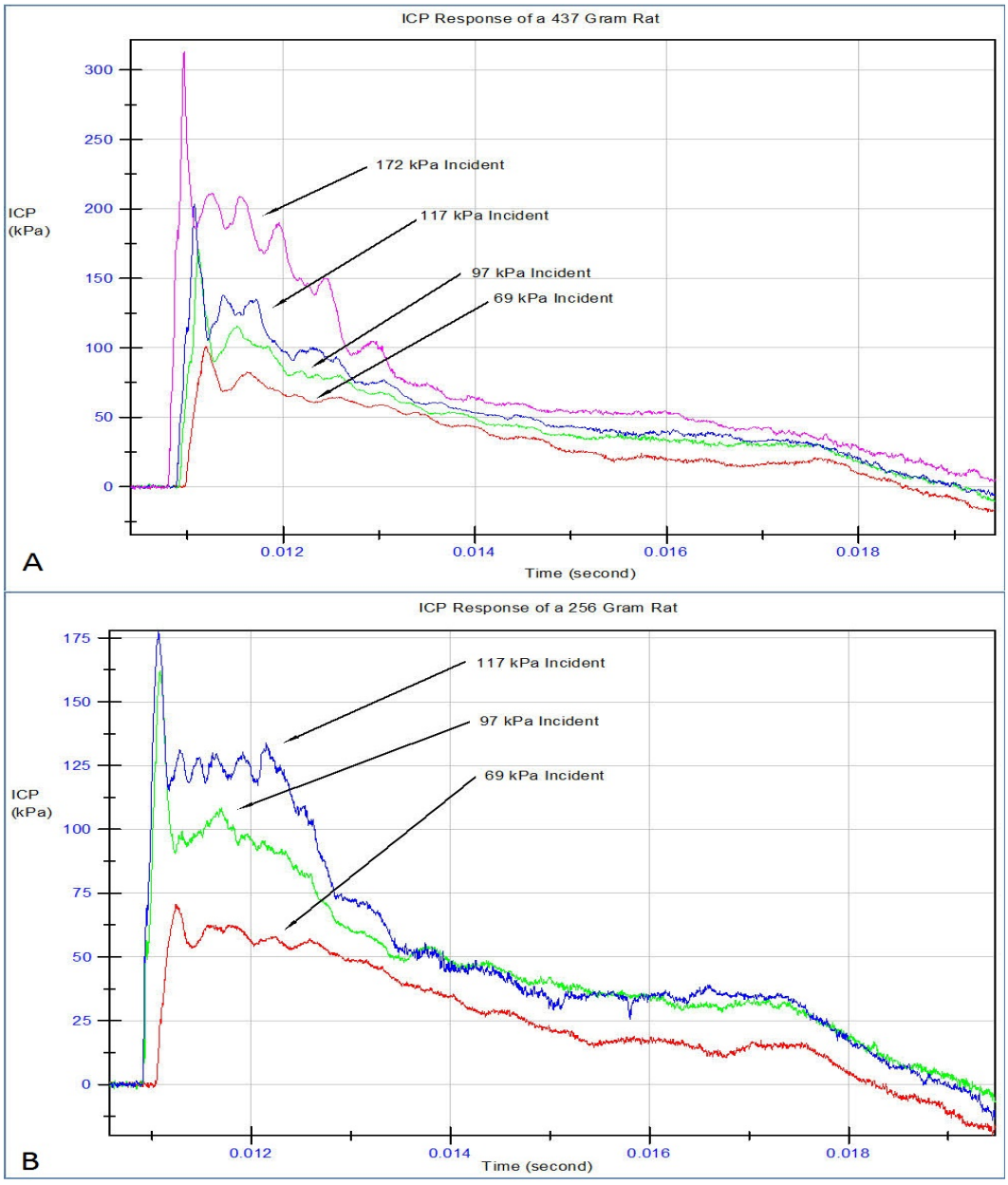

Figure 3. Intracranial pressure measurements with the fiber optic pressure sensor mounted on the top of the skull. For the 437 gram rat (A) the most uninhibited high frequency waveform was excited at the 172 kPa incident intensity. For the 256 gram rat (B) the frequency emerged when the 117 kPa incident shock wave was introduced.

At a specific intensity, seeming to be partially dependent on rat weight, the high frequency waveform would oscillate the most uninhibited. The 256 gram rat oscillated the most freely during a 117 kPa incident shock, and the 437 gram rat oscillated the most freely during a 172 kPa incident shock The OIC group pressure response for a 232 gram and 317 gram rat are provided in Figure 4.

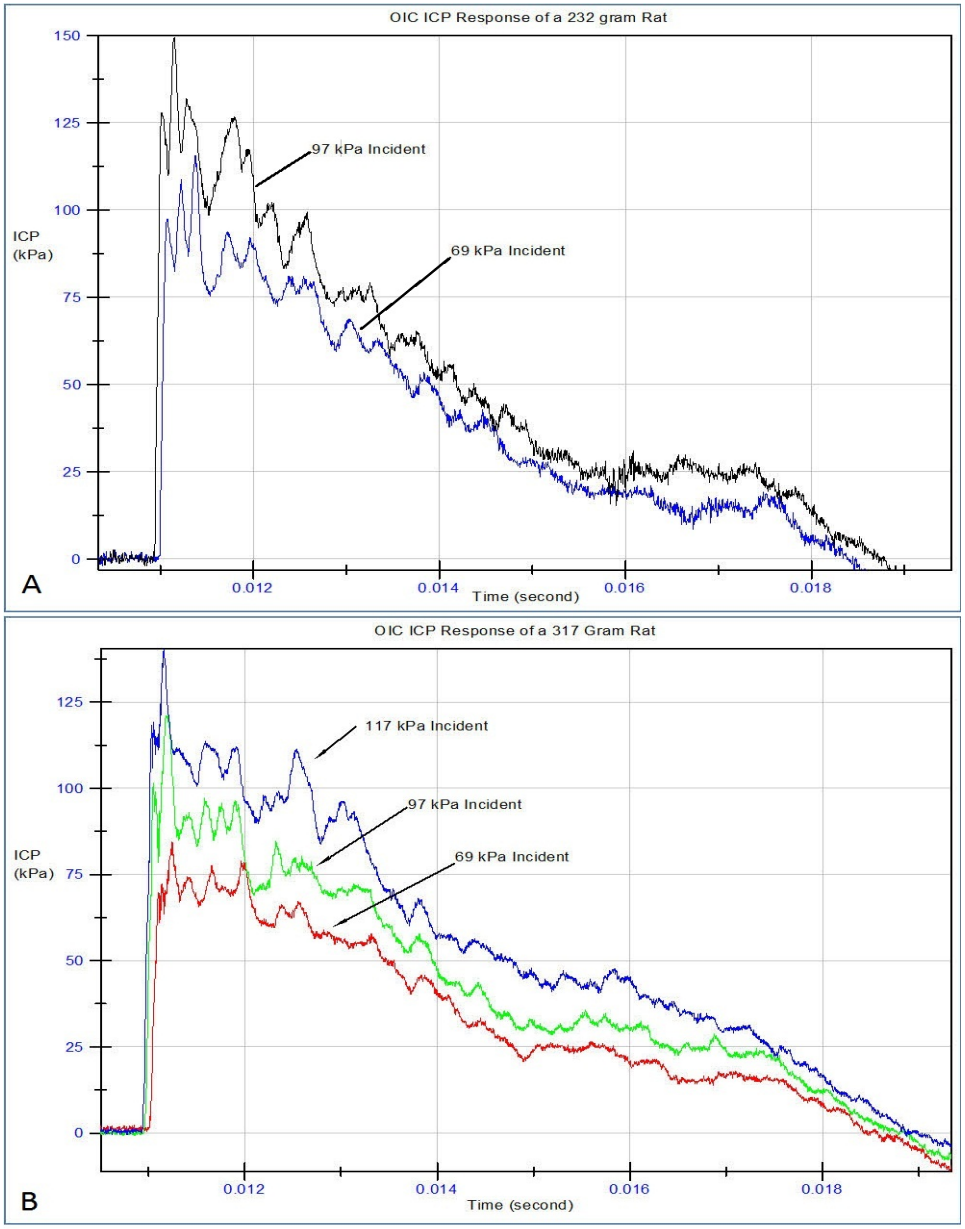

Figure 4. The OIC instrumented rats report higher frequencies but show similar results to the IC rats. The 232 gram rat (A) demonstrated high levels of excitation at the 69 kPa intensity. The 317 gram rat (B) responded the most ideally at the 97 kPa intensity. For the 317 gram rat, the 117 kPa intensity response tends to return to a less predictable waveform.

Without instrumentation on the external superior aspect of the skull, pressure oscillations were still measured within the brain, but were present at greater frequencies. For the 232 gram rat the 69 kPa incident shock excited the event, whereas the 97 kPa incident excited the 317 gram rat. The peak pressure amplitude measured in the rats was shown to linearly increase with ambient pressure intensity. For both group 1 ($p < 0.0001$) and group 2 ($p < 0$ .0001), the data indicated that the maximum ICP response of each population was significantly different to each other when grouped by incident intensity. During investigation of the ratio of the peak intracranial pressure to the peak ambient pressure, it was found that the 172 kPa and 69 kPa incident shock wave exposed in the IC group were significantly different than the 97 kPa and 117 kPa exposed rats (Figure 5). This suggests that the ratio of peak ICP/ peak ambient increases with intensity for the IC group. No significant differences were measured for the OIC group. Weights were not normalized during this process.

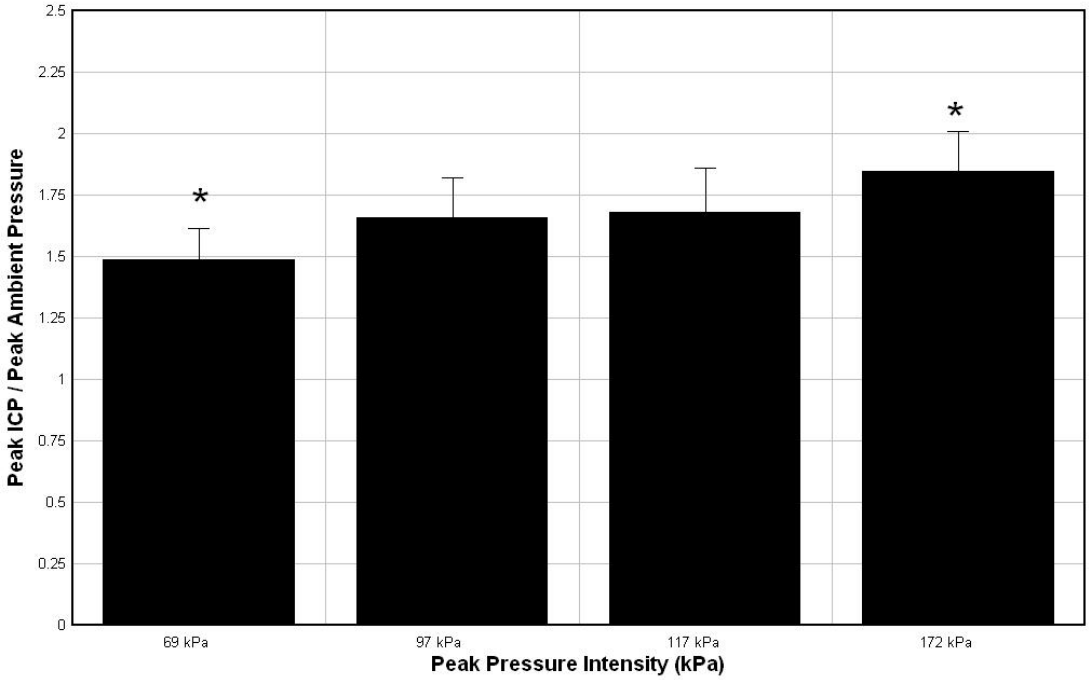

Figure 5. The ratio of peak ICP and peak ambient pressure was calculated. For the IC group, it was shown that as the intensity increases the ratio of peak ICP to peak ambient increases as well. The 172 kPa and 69 kPa groups were significantly different than the 97 kPa and 117 kPa groups (* $p < .05$).

The calculated frequencies from the IC group were analyzed. The rat weight, incident shock intensity, and frequency were all compared. The data indicated that as the rat weight and shock wave intensity increased, the calculated frequency decreased for the IC group. The calculated frequency for the OIC group was 7030 ± 1341 Hz and frequency results for the IC group were 4984 ± 1316 Hz.

1.4. Discussion of top mounted versus back mounted sensors

From this study, it has been demonstrated that the skull acts as an interface between the shock wave and the brain. This phenomenon has been demonstrated by the modification of either the superior or posterior brain case. For the IC group, it was shown that as a rat became heavier, the secondary signal would oscillate at lower frequencies and that greater incident shock wave intensities were required to invoke this oscillatory response. The response appeared to be similar to that of a damped harmonic oscillator. Where there would be an initial deflection and then a series of oscillations that would dampen out and return to pre-event conditions.

Instrumentation placement appeared to alter the frequency of the pressure oscillations within the brain. Factors associated with those modifications included the additional mass and stiffness on the surface of the brain case from the application of bone cement and equipment for mounting the pressure sensor.

To address the issues associated with instrumenting the top of the skull, the fiber optic sensor was mounted into the occipital bone to measure the intracranial pressure response without changing the native properties of the superior surface. The results indicated that mounting of instrumentation to the superior surface did have an effect on the observed oscillatory response. In both groups, intracranial pressure peaks increased with intensity, but the increase in the ratio of the ICP to ambient pressure peaks was specific to the IC group data. A limitation to the instrumentation of the OIC group, however, was that the animals were sacrificed prior to testing due to the severity of the surgical procedure. As such, they may not have had the same baseline intracranial pressures as the animals from the IC group which were alive when testing.

It has been determined that the skull plays a significant role in determining the pressure profiles that develop in the brain. Mounting the pressure sensor on the top of the skull or testing with heavier rats resulted in changes to the frequency content of the system during shock wave exposure. If the mechanical properties of the skull are able to dictate the imparted pressure profiles in the brain, then the neurological response of the rat may be predicted by that exposure. This is reinforced by the results that the frequency and expression of the oscillations that developed are specific to intensity. If the measured oscillations are related to the formation of compression waves by skull flexure, there could be specific pressure intensities the lead to exaggerated neurotrauma in the rat.

VandeVord *et al.* (2011) recently demonstrated that rats would exhibit exaggerated cognitive declines and neuropathological increases at a specific band of pressures (VandeVord *et al.* 2011). The most exaggerated trauma for the rats (average weight ~ 300 grams) was around 117 kPa. When exposed to greater intensities the rats would experience less of the cognitive declines. It is hypothesized that the rats may be injured to a greater degree when the peak oscillation phase becomes the most dominate. Additional studies will need to be undertaken to confirm this association.

The ICP data was of use because it has helped explain how sensitive the rat skull is to blast. Either by increasing the weight of the specimen or changing the mounting of the sensors,

the imparted waveform will change. This is important to understand because the rat may be much more sensitive to a shock wave exposure than the other models of blast.

2. STUDYING SKULL MOTION WHEN HEAD IS EXPOSED TO SHOCK WAVE.

Although there has been a rise in the number of blast neurotrauma reports, the exact mechanism of how the brain is injured remains a topic of debate (Bolander et al. 2011; Cernak et al. 2001; Clemedson 1956; Clemedson and Jonsson 1961; Courtney and Courtney 2009; Dal Cengio Leonardi et al. 2011). Proposed theories on the mechanism of damage vary from transosteal propagation (Clemedson 1956; Clemedson and Jonsson 1961), which hypothesized that the shock wave enters the brain by propagating directly through the skull, to a thoracic mechanism, by which the overpressure squeezes the thorax and transmits pressure to the brain through the vasculature (Cernak et al. 2001; Courtney and Courtney 2009). Studies that had the ability to measure intracranial pressure (ICP) indicated that there was little evidence to support a significant transmission of pressure through the body vasculature (Clemedson 1956; Dal Cengio Leonardi 2011; Romba and Martin 1961; Saljo et al. 2008). Furthermore, these studies confirm that transosteal propagation is unlikely since the ICP amplitudes are not diminished by the impedance mismatch.

Most recently, our experimental studies have investigated the biomechanical response of the head exposed to a shock wave. The results indicate that the imparted shock wave may induce multiple response modes of the skull, including global flexure, which may have a significant contribution to the mechanism of injury (Bolander et al. 2011; Dal Cengio Leonardi et al. 2011).

In order to better describe the biomechanical response of the head to a shock wave, we measured skull strain and deformation during shock wave exposure.

2.1. Methods of measuring strain and ICP.

In this series of tests, rats were exposed to shock waves of increasing intensity. The first set of tests investigated the relationship between skull strain and intracranial pressure (ICP). The goal was to provide an overall understanding of rat head response to shock wave exposure. Approval of all experiments was obtained from the Wayne State University Institutional Animal Care and Use Committee (IACUC) prior to testing. A total of ten male Sprague Dawley rats, age 65-70 days old, were procured. All animals were given food and water ad lib. Animals were randomly assigned to one of two groups based on instrumentation used during the testing: strain gage (SG) or intracranial pressure sensor mounted to the top of the skull (IC).

Five SG rats were sacrificed immediately prior to testing. The dermal tissue was removed from the medial dorsal surface of the head exposing a 1.5cm wide region of the skull extending from 1-cm rostral to the bregma to 1-cm caudal to the lambda. The skull surface was then cleaned using acetone to ensure a solid and durable mechanical bond with the strain gage. A three-axis

rectangular Rosette-style strain gage (FAER-25B-35SX, Vishay micro measurements) was then attached to the skull surface using cyanoacrylate and allowed five minutes to cure. To limit motion of the rat's head during exposure and prevent mechanical stress on the instrumentation wires, the nose was secured such that the head was pitched down at approximately 45 degrees to the shock front. The channels were named rostral, medial, and caudal (Figure 6).

Five IC-designated rats were anesthetized using a ketamine/xylazine mixture (80mg/kg/10 mg/kg; I.P) and immobilized in a stereotaxic frame. A longitudinal incision was made along the dorsal medial surface of the head, exposing the skull from the bregma to the lambda. A 1.5mm diameter hole was drilled using a stereotaxic high-speed drill at the following location: +3.0 (A-P (mm) from Bregma), -2.0 (M-L (mm)), and -1.0 (D-V (mm)), exposing the frontal cortex.

A plastic guide cannula (18-gage; 1.2 mm, CMA Microdialysis, Sweden) with a small pedestal was implanted through the hole and fixed to the skull using two small stainless steel screws inserted at 45 degree angles from the horizontal into the skull adjacent to the cannula. Cranioplastic cement was applied to fix the pedestal to the skull and was anchored by the screws. The surgical wound was closed with sutures, as needed. A dummy cannula insert with a threaded cap was inserted in the guide cannula until shock exposure; the rats were allowed five days recovery time.

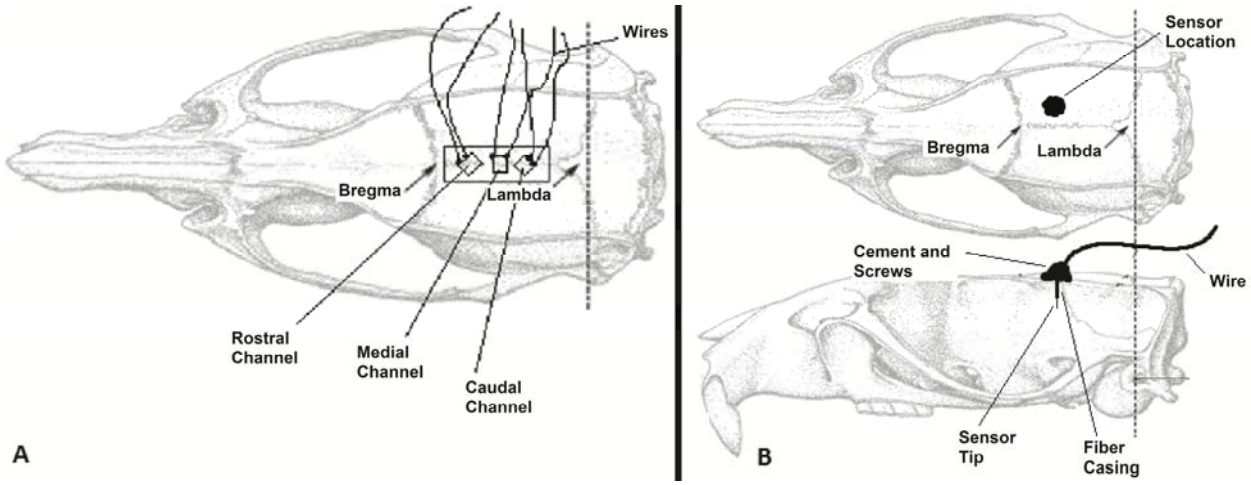

Figure 6. Placement of strain gage on surface of the rat skull (A) and fiber optic pressure sensor installation on a rat skull (B).

Prior to testing, rats were anesthetized using ketamine/xylazine mixture (80mg/kg/10 mg/kg; I.P). The cannula was then filled with a sterile saline solution. The cannula cap was filled with petroleum jelly and a fiber optic pressure sensor (FOP-MIV, FISO Inc.) was inserted into the cannula and threaded onto the cannula pedestal. Figure 6B provides a sketch of the technique applied.

The rat was affixed to a trolley-mounted stage using a nylon harness, and inserted into the shock tube, such that its nose was positioned 114 cm inside the end of the Lexan® tube opposite

to, and facing, the driver (Figure 7). The harness maintained the rat's longitudinal axis perpendicular to the shock front and in fixed proximity to a side-on pressure sensor. The trolley system reduced the effects of post-shock dynamic pressure flow on the rat.

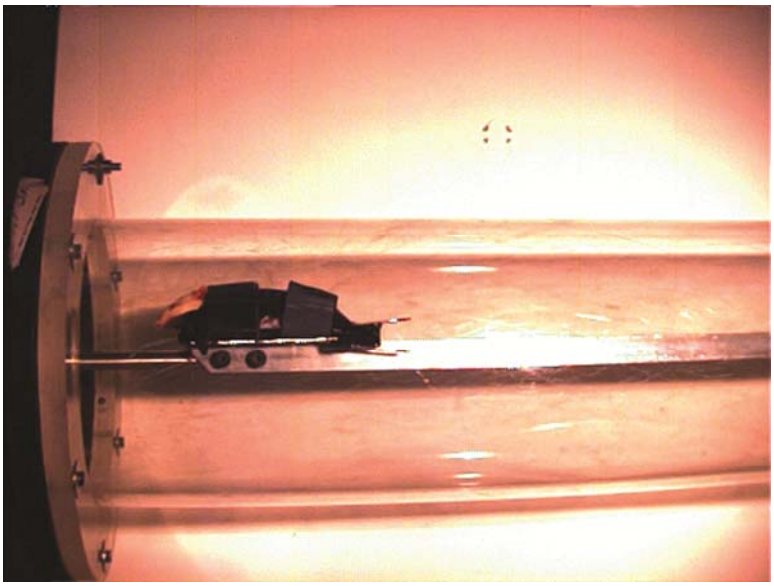

Figure 7. The rat was placed 114 cm within the shock tube and was placed on a trolley system to reduce the level of dynamic pressure shifts that are not representative of a free-field shock wave.

Once placed in the harness, the SG rats were subjected to three exposures each at 69, 97, 117, and 172 kPa incident shock pressure or until sensor failure, thus a total of 12 exposures per animal. The IC rats were exposed to three repeated exposures at three intensities (69, 97, and 117 kPa). In order to conserve the integrity of the ICP sensors, the highest pressure intensity (172 kPa) was not applied. The intensities used in the protocol were determined from previous tests to maximize the amount of useful data. The time in between exposures was approximately two minutes for both groups of animals.

Both ICP and strain data were collected at 400 kHz using the Dash 8HF data acquisition system (Astro-med Inc). The data was then post-processed completed using Diadem 11.0 (National Instruments). Calculations of maximum principal strain (Equation 1) were made using the formula below; the rostral gage measured ε1, the medial gage, ε2, and the caudal gage, ε3.

$$\varepsilon_{P,Q} = \frac{\varepsilon_1 + \varepsilon_3}{2} \pm \sqrt{\left[(\varepsilon_1 - \varepsilon_2)^2 + (\varepsilon_2 - \varepsilon_3)^2 \right] / 2} \quad (1)$$

The data were reported in microstrain and the magnitude of the first compressive peak was recorded. The peak intracranial pressure was also recorded. The wave profiles from the ICP sensors were then differentiated so that rate of pressure change could be calculated and

compared. Data were grouped by incident shock wave intensity and responses were compared using ANOVA with *post hoc* Tukey HSD used to determine significant differences ($p < 0.05$) between groups.

2.2. Results of SG Measurements

The data collected from the strain gages were useful for determining the flexural response of the superior braincase to shock wave loading. There were characteristic superimposed response patterns that were observed consistently as follows: (1) A strong and rapid compression with an associated damped oscillation at relatively high frequency (less than 3kHz). (2) A quasi-steady decompression closely following the decay of the external static overpressure condition that developed as the strain returned to pre-blast levels. (3) A waveform of lower frequency with its pulse beginning in tension following the rapid compression. These responses were present for all the rats tested (Figure 8).

The waveforms from two different rats are presented in Figure 8, and the characteristic responses described prior are observable for both series. The first trace in each series is from the side-on (static) pressure sensor exposed to the incident shock wave. Within both series, following the incident shock, reflections from the fixture holding the specimen develop and create pressure artifacts on the sensor's surface that are not representative of the environment to which the specimen is exposed. This effect is expected from theory; the arrival and amplitude of the perturbation coincides with those expected of that reflection disturbance; confirmation of this phenomenon is also demonstrated by the fact that the shock reflections are similar between series, while the strain response is specific to the specimen being tested.

The peak compression was reported for all exposures. In Figure 9 A, it is shown that as the incident shock wave intensity increases, the calculated maximum principal strain also increased for the rats instrumented with strain gages. The means were signifcantly different between exposure intensities ($*p < 0.05$).

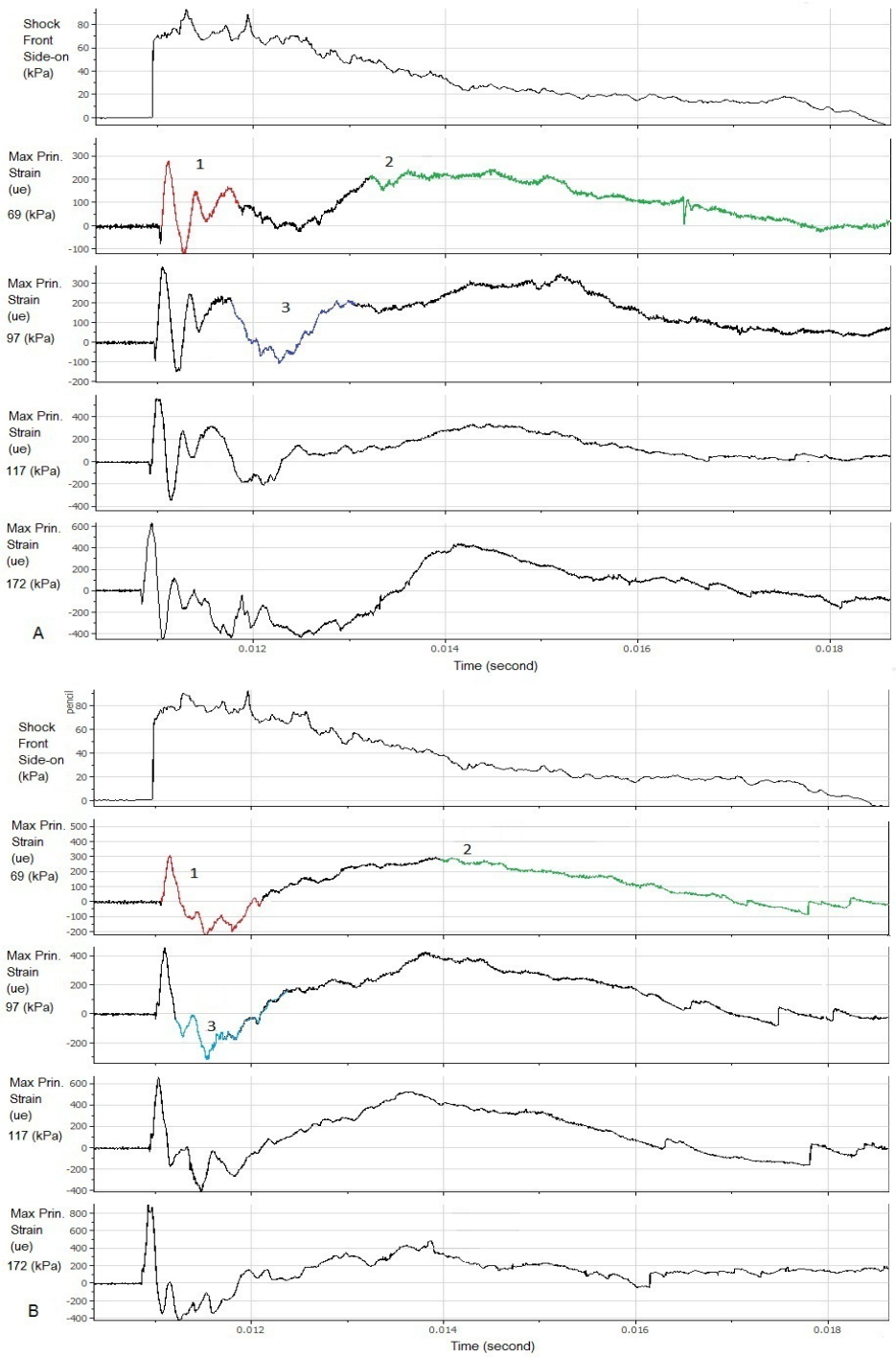

Figure 8. Principal strain response profiles of the superior brain case for both a 262 and 247 gram rat when exposed to shock waves of increasing intensity. For the presented data, tension is positive and compression is negative. (1) (red) A strong and rapid compression with an associated damped oscillation at relatively high frequency somewhat less than 3kHz which increases slightly with shock intensity . (2) (green) As this oscillatory response would dampen out, a quasi-steady decompression closely following the decay of the external static overpressure. (3) (blue) A much lower frequency pulse beginning in tension that followed the incident shock.

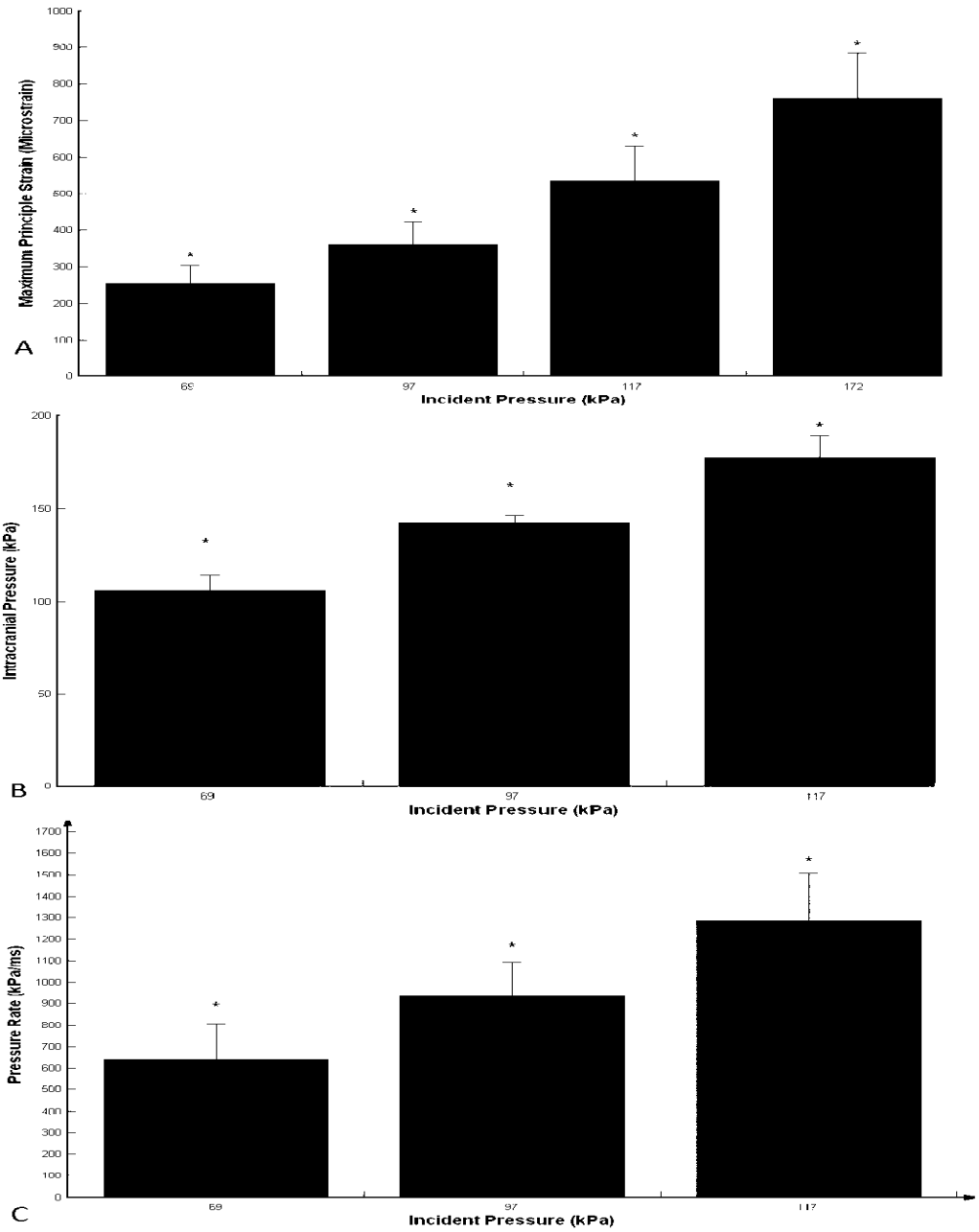

Figure 9 (A) The initial compression of the skull is dependent on intensity of the incoming shock wave. The largest magnitude shock waves caused the greatest maximum principal strains for rats instrumented with strain gages. The response of the rats, separated by exposure intensity, were significantly different for each exposure intensity level (* p <0 .05). (B) The ICP will increase beyond that of the incident shock wave (* p <0 .05) for rats instrumented with ICP sensors. (C) The rate of pressure change will also increase with intensity (* p<0 .05).

2.3. Results of ICP measurements

For the intracranial pressure profiles, two response patterns were observed consistently between specimens. (1) The peak compression wave will rebound and oscillate in a dampened harmonic motion. (2) There was a rapid increase in pressure that approximates the external loading environment and then return to pre-exposure conditions. In Figure 9B and C it is shown that as the incident shock wave intensity increased, the peak pressure and maximum rate of pressure change both increased.

The pressure response profiles for a 249 gram rat are shown in Figure 10. The three profiles have been time shifted to begin at the same point. The increase in peak pressure as a function of an increase in incident pressure can be observed for this series of waveforms. The duration of the rise times is also a function of intensity, where the greatest intensities resulted in the shortest rise times.

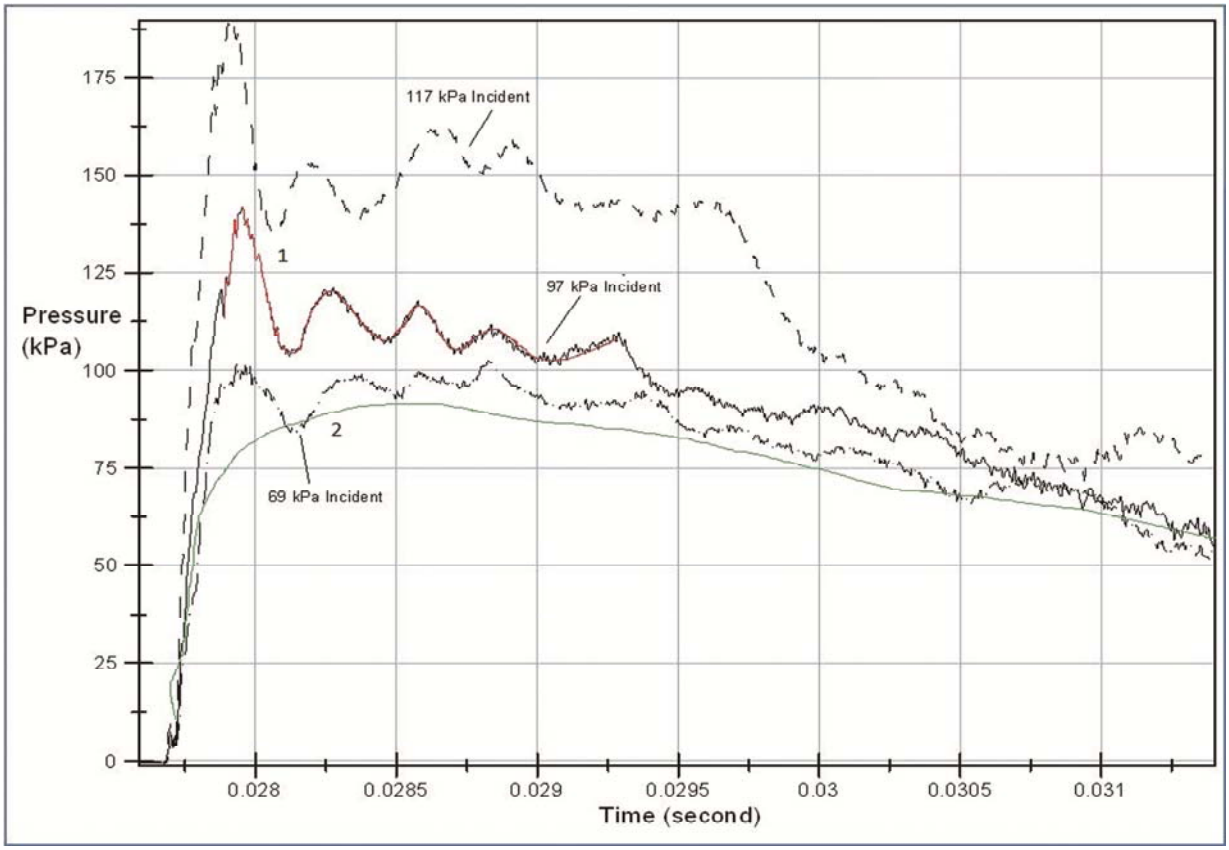

Figure 10. The intracranial pressure response of a rat is dependent on shock wave intensity. The ICP responses for a 249 gram rat show distinct pressure fluctuations (1) (red) that are present in each of the profiles that last for less than two milliseconds and are similar to those observed in the strain gage response. The waveforms also undergo a quasi-steady compression response that approximates the external loading response invoked by the shock wave (2) (green).

To further this point, the 97 kPa ICP wave form was time shifted so that its pressure profile could be compared to a 97 kPa incident shock wave without the shock reflections that were observed in Figure 10 (Figure 11). The rise times between the incident wave on the external pressure sensor and the intracranial pressure wave is of interest (27 compared to 195 microseconds).

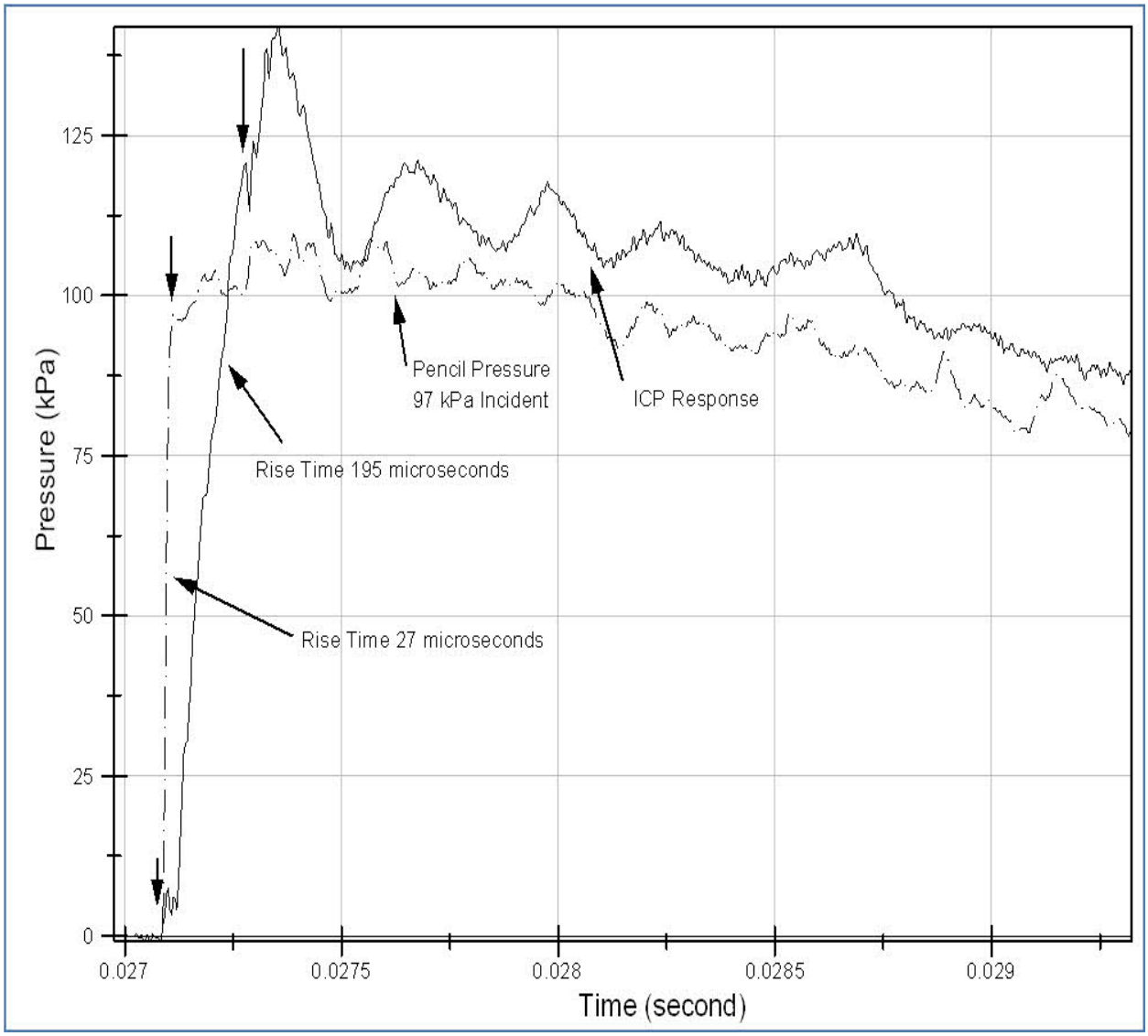

Figure 11. The rise time of the external pressure wave is faster than the rise time of the record intracranial pressure for the ICP recording of a 249 gram rat.

2.4. Discussion of strain and ICP biomechanical results

Recent experimental biomechanical data for the rat suggested that skull flexure contributes to the intracranial pressure gradients developed within the brain as a result of shock wave interactions. Results from the current experiments validate the hypothesis by Leonardi et al. (2011) demonstrating that strain on the skull surface may have a significant effect on the imparted ICP waveform. Through a series of pressure intensity exposures, it was observed in this study that the ICP response was dependent on the incident shockwave intensity. Further, the rate of pressure change was found to increase while the rise time to peak pressure was found to decrease with intensity.

When the ICP response was compared to the pressure profile of the incident shock wave, a delay in the rise time of the ICP was observed. This suggests that the rat skull is acting as a medium between the external environment and the intracranial contents. Pressure recordings reported by (Bauman et al. 2009) also found a significant delay in the rise time of the ICP profile compared to the incident shock wave during their swine testing. It is hypothesized that the rise time of those ICP profiles within the swine will be longer than that of the rat because of the difference in skull thickness between species. More studies need to be conducted in order to verify this relationship.

The results from the strain gage data further substantiates the hypothesis that the incident shock wave is causing the skull to flex. The rapid compression that increases in magnitude with the intensity of the incident shock is believed to be the direct result of the shock wave compressing the skull surface. The damped harmonic oscillation phase that then developed as a result of the compression is hypothesized to be due to the return of the deflected surface regions back to equilibrium. The quasi- steady decompression phase that approximates the external pressure environment is then best observed due to the dispersion of the energy from the rapid compression of the skull case. The nature of the secondary surface wave beginning in tension has yet to be determined. It has been observed that this wave is dependent on the intensity of the incident shock wave. The front of this wave will be steeper as the intensity increases. Research is ongoing to determine the nature of this wave.

Because of these observations in both the strain gage and intracranial pressure responses, it is proposed that there are two major regions in the wave form response. The first is the transient phase which consists of a rapid compression and harmonic oscillations; the other is the quasi-steady decompression phase. It is possible that the most damaging aspect of these waveforms is the initial oscillations that may cause high levels of strain rates in both tension and compression that could be transferred as rapid compression waves within the brain due to the coupling at the skull/dura interface.

Some limitations exist with the current data. The placement of the strain gage on the skull is problematic because mounting on the suture lines will cause an amplification of the signal. Although the results provided key information, the principal strain calculations were not made on a homogenous surface and the sensors were relatively widely distributed. But, given

the consistency of the signals between exposures and that similar responses were observed between species, the data are useful for describing responses of the rat skull to shock wave exposure.

The ICP data were of concern because the skull was modified with small screws and bone cement, modifying the native surface. If the superior skull case is acting as a diaphragm, the additional mass of the sensor cement complex will cause the periodic oscillations to have a response with less competing frequencies that what are observed in the strain profiles Additionally, it still needs to be determined to what extent the fiber optic sensors are mapping the motion of the skull when compared to the environment within the brain. Because of the artifacts of testing with the ICP sensors, direct relationships were not made to the strain gages.

KEY RESEARCH ACCOMPLISHMENTS

- We demonstrated that the skull acts as an interface between the shock wave and the brain.
- As a rat became heavier/more mature, the secondary signal would oscillate at lower frequencies and that greater incident shock wave intensities were required to invoke this oscillatory response.
- Instrumentation placement appeared to alter the frequency of the pressure oscillations within the brain. Factors associated with those modifications included the additional mass and stiffness on the surface of the brain case from the application of bone cement and equipment for mounting the pressure sensor.
- We developed a new method for ICP recordings to address the issues associated with instrumenting the top of the skull. The new method includes a fiber optic sensor which is mounted into the occipital bone to measure the intracranial pressure response without changing the native properties of the superior surface.
- New instrumentation method indicated that mounting of instrumentation to the superior surface did have an effect on the observed oscillatory response.
- The results from the strain gage data further substantiates the hypothesis that the incident shock wave is causing the skull to flex. The rapid compression that increases in magnitude with the intensity of the incident shock is believed to be the direct result of the shock wave compressing the skull surface.
- First manuscript was accepted for publication in the Journal of Neurotrauma (Impact factor = 4.25)
- Second manuscript was accepted for publication in the Annals of Biomedical Engineering (Impact factor = 2.4)
- Drafting third manuscript on orientation effects which we plan to submit by the end of December (2011)

REPORTABLE OUTCOMES

Publications:

1. Leonardi AC, Bir CA, Ritzel D, VandeVord PJ. Intracranial pressure increases during exposure to a shock wave. *J Neurotrauma*. Jan;28(1):85-94 (2011)
2. Bolander R, Mathie BA, Bir CA, Ritzel D, VandeVord PJ. The Contribution of Skull Flexure as a Possible Mechanism for Neurotrauma in the Rat when Exposed to a Shock Wave. *Annals of Biomedical Engineering*; Accepted (2011)

3. Leonardi AC, Keene N, Bir CA, VandeVord PJ. Head Orientation Affects the Intracranial Pressure Response Resulting from Shock Wave Loading in the Rat. Planned submission to Journal of Neurotrauma, Nov 2011.

Poster Presentations:

1. *Bolander R, Bir CA, VandeVord PJ. Maturation related changes may explain a range specific response in the rat model to shock wave induced neurotrauma**.*** *The Eight World Congress on Brain Injury,* Washington DC. March 2010.

   Awarded first place poster presentation.
2. Dal Cengio AL, Ritzel D, VandeVord PJ. Cranial Flexure as a Primary Mechanism for Blast-TBI. *Proceedings for the National Neurotrauma Society*. Las Vegas, NV, July 2010.
3. Mathie BM, VandeVord PJ. Variances in the Blast-Induced Intracranial Pressure Response Due to Subject Orientation. *Advanced Technology Applications for Combat Casualty Care,* St. Petersburg, FL, August 2010.
4. Mathie BM, VandeVord PJ. Variances in the Blast-Induced Intracranial Pressure Response Due to Subject Orientation. *Biomedical Engineering Society Annual Meeting,* Austin, TX, October, 2010.

CONCLUSIONS

There is a pressing need for a comprehensive explanation of the mechanism of traumatic brain injury after exposure to blast, and the testing of animals instrumented with pressure sensors in the brain is becoming increasingly important. It is of paramount importance to conduct tests in a way that will maximize the attainment of dependable results and minimize the sacrifice of animals. Historically, some animal tests have been designed and carried out in an attempt to learn more about the mechanism of shock wave transmission to the brain, but only a few animal studies recorded direct pressure within the brain tissue during exposure to blast (Chavko 2007; Clemedson 1956; Clemedson 1961a and b; Romba 1961). In fact such experiments are challenging to setup because the instrumentation technology, which measure the true in vivo pressure condition during shock exposure, has not yet been perfected and validated. Furthermore animal tests carry the burden of the complex preparation of the animals in addition to the strict guidelines for animal handling. Our previous results were the first to demonstrate that seemingly minor unsealed apertures through the skull such as those that might be made for insertion of gauges, can significantly affect ICP measurements. Once the skull was sealed, we noticed a ***significant increase*** in ICP during blast. **These findings have been recently published in the high impact factor *Journal of Neurotrauma* (Leonardi et al 2011)**.

The progression we made this past year will again have a large impact in the area of blast neurotrauma. Made clear by the series of tests presented is the sensitivity of the brain-skull system to shock waves. Investigating the effect of instrumentation and conducting further

biomechanical tests to measure strain on the skull have provided important information to the scientific community. The data has provided key evidence that skull flexure is a likely candidate for the development of ICP gradients within the rat brain. **These findings have been recently published in the high impact factor *Annals of Biomedical Engineering* (Bolander et al 2011)**.

REFERENCES

Bauman, R. A., G. S. Ling, L. Tong, A. Januszkiewicz, D. Agoston, N. Delanerolle, J. Kim, D. Ritzel, R. Bell, J. M. Ecklund, R. Armonda, F. Bandak and S. Parks. (2009). An introductory characterization of a combat-casualty-care relevant swine model of closed head injury resulting from exposure to explosive blast. J Neurotrauma. Jun;26(6):841-860.

Bolander R, Mathie BA, Bir CA, Ritzel D, VandeVord PJ. (2011). The Contribution of Skull Flexure as a Possible Mechanism for Neurotrauma in the Rat when Exposed to a Shock Wave. Annals of Biomedical Engineering; Accepted

Celander HC, CJ. (1954). The use of a compressed air operated shock tube for physiological blast research. Acta Physiologica Scandinavica 33(1):6-13.

Cernak, I., Z. Wang, J. Jiang, X. Bian and J. Savic (2001). "Cognitive deficits following blast injury-induced neurotrauma: possible involvement of nitric oxide." Brain Inj 15, 593-612.

Chavko M. (2007). Measurement of blast wave by a miniature fiber optic pressure transducer in the rat brain. Journal of Neuroscience Methods 159(2):277-281.

Clemedson CJ. (1956). Shockwave transmission to the central nervous system. Acta Physiologica Scandinavica 37(2-3):204-214.

Clemedson CJ, A. (1961a). Transmission of elastic disturbances caused by air shock waves in a living body. Journal of Applied Physiology 16(3):426-430.

Clemedson CJ, Jonsson, A. (1961b). Transmission and reflection of high explosive shock waves in bone. Acta Physiologica Scandinavica 51:47-61.

Courtney, A. C. and M. W. Courtney (2009). A thoracic mechanism of mild traumatic brain injury due to blast pressure waves. Med Hypotheses 72, 76-83.

Leonardi AC, Bir CA, Ritzel D, VandeVord PJ. (2011). Intracranial pressure increases during exposure to a shock wave. *J Neurotrauma*. Jan;28(1):85-94.

Romba JJM, Paul. (1961). The propagation of air shock waves on a biophysical model. In: Laboratories UAOHE, editor. Aberdeen Proving Ground, Maryland: Armed Services Technical Information Agency. p 1-25.

Saljo, A., F. Arrhen, H. Bolouri, M. Mayorga and A. Hamberger (2008). Neuropathology and pressure in the pig brain resulting from low-impulse noise exposure. J Neurotrauma 25, 1397-1406.

VandeVord PJ, Bolander R, Sajja VS, Bir CA. (2011). Mild Neurotrauma Indicates a Range Specific Pressure Response to Low Level Shock Wave Exposure. *Annals of Biomedical Engineering*; Accepted

APPENDIX

1. Bolander R, Mathie BA, Bir CA, Ritzel D, VandeVord PJ. The Contribution of Skull Flexure as a Possible Mechanism for Neurotrauma in the Rat when Exposed to a Shock Wave. *Annals of Biomedical Engineering*; Accepted (2011)

Annals of Biomedical Engineering, Vol. 39, No. 10, October 2011 *(© 2011)* pp. 2550–2559
DOI: 10.1007/s10439-011-0343-0

Skull Flexure as a Contributing Factor in the Mechanism of Injury in the Rat when Exposed to a Shock Wave

RICHARD BOLANDER,[1] BLAKE MATHIE,[1] CYNTHIA BIR,[1] DAVID RITZEL,[2] and PAMELA VANDEVORD[1,3]

[1]Department of Biomedical Engineering, Wayne State University, 818 W Hancock, Detroit, MI 48201, USA;
[2]Dyn-FX Consulting Ltd., 19 Laird Ave N, Amherstburg, ON N9V 2T5, Canada;
and [3]John D Dingell VAMC, Detroit, MI 48201, USA

(Received 6 April 2011; accepted 23 June 2011; published online 7 July 2011)

Associate Editor Stefan M Duma oversaw the review of this article.

Abstract—The manner in which energy from an explosion is transmitted into the brain is currently a highly debated topic within the blast injury community. This study was conducted to investigate the injury biomechanics causing blast-related neurotrauma in the rat. Biomechanical responses of the rat head under shock wave loading were measured using strain gauges on the skull surface and a fiber optic pressure sensor placed within the cortex. MicroCT imaging techniques were applied to quantify skull bone thickness. The strain gauge results indicated that the response of the rat skull is dependent on the intensity of the incident shock wave; greater intensity shock waves cause greater deflections of the skull. The intracranial pressure (ICP) sensors indicated that the peak pressure developed within the brain was greater than the peak side-on external pressure and correlated with surface strain. The bone plates between the lambda, bregma, and midline sutures are probable regions for the greatest flexure to occur. The data provides evidence that skull flexure is a likely candidate for the development of ICP gradients within the rat brain. This dependency of transmitted stress on particular skull dynamics for a given species should be considered by those investigating blast-related neurotrauma using animal models.

Keywords—Blast, Injury, Mechanism, Explosion.

INTRODUCTION

Due to the current military campaigns and social unrest around the world, the exposure of humans to explosions continues to take place.[10,11,15] A classification system has been invented to describe the manner in which a specific pathology will develop as a result of the trauma caused by the explosion.[12,13,16] The manner in which the shock wave from the explosion causes trauma (primary blast injury) remains a major concern to researchers investigating this injury pattern because of its ambiguous nature.[19]

Multiple hypotheses describing how this injury may result have been suggested. Courtney and Courtney[7] have recently summarized the major hypotheses of the mechanism of primary blast injury. One hypothesis is that the blast wave will compress the thorax and a resulting pressure surge to the head will cause brain injury.[1,3] This hypothesis has been discussed as early as 1916.[18] A second injury mechanism that is hypothesized states that a combination of rotational and translational accelerations resulting from shock wave interaction with the head will be great enough to cause injury.[8,21]

A third hypothesis provided by Courtney and Courtney[7] involves the transmission of the blast energy directly through the cranium. However, the physics of direct stresswave transmission should be distinguished from waves imparted by skull flexure. Direct wave transmission (trans-osteal wave propagation) in this case concerns the processes by which an air-borne shock wave interacts with the material interface of the skull and transmits a 'through-thickness' stress by direct compression of the skull material. The deformations caused by this mode of energy transfer will result in high frequency, low amplitude perturbations, similar to acoustic transmission. The development of the reflected pressure on the skull surface can also transmit enough energy to cause skull flexure. This deformation, in turn, may also cause changes in the pressure environment within the brain. Computer models have observed this transmission of blast energy in humans, but have yet to validate the results against experimental data.[4,17,22]

Courtney and Courtney[7] reference the work from Chavko *et al.*[5] which reports that ICP records within the cranium are very similar in pressure to the external

Address correspondence to Pamela VandeVord, Department of Biomedical Engineering, Wayne State University, 818 W Hancock, Detroit, MI 48201, USA. Electronic mail: dt8583@wayne.edu, blakemathie@gmail.com, cbir@wayne.edu, dritz@dyn-fx.com, pvord@wayne.edu

static pressure condition. However, Leonardi *et al.*[14] compared records from unsealed and completely sealed intracranial pressure (ICP) sensors from rodents exposed to a shock wave which indicated that the observation by Chavko may have been an artifact of an unsealed ICP gauge. The study by Leonardi *et al.* indicated that by creating a fully sealed testing environment, mimicking the actual physiological environment, peak ICP profiles exceeding the external static pressure environment will develop. The unsealed environment produced similar recordings to those of the external pressure measurements since the enhanced fluid pressurization was able to be relieved through the leaking seal. They also noted distinct ICP oscillations taking place in the signal following the initial pressure rise, the amplitude, and frequency of the imparted ICP was likely linked to skull dynamics.

Other researchers have also observed an oscillatory ICP response following an initial rise in pressure, with the response depending on the dampening of the tissues tested.[6,20] In order to determine the source of ICP oscillations, Romba and Martin[20] investigated the effect of shielding the thorax of the Rhesus monkey while subjecting the head to blast exposure. Their results indicated that ICP oscillations were found regardless of the presence of thorax protection. Recently, similar results demonstrated that strong blast-induced ICP was inflicted in swine despite being fitted with thoracic protection.[2] A pressure pulse was generated in the inferior vena cava during exposure, but the delay was approximately two ms with a much longer rise time to peak pressure. Additionally there was no parallel increase in the ICP profiles relative to this pulse.

In the case of head exposures to shock waves, it is hypothesized that the dynamic structural response modes of the skull, with the associated viscoelastic brain mass acting as a coupled mechanical system, controls the stress (pressure) imparted to brain tissue under shock wave loading. The dynamic response modes of the skull, and hence imparted ICP, will relate to its particular geometry and material characteristics.

An experiment was designed to confirm this hypothesis will provide valuable information to identify particular modes of the coupled skull/brain response and their correlation with the ICP waveforms developed. Components of the imparted high strain rates in the form of ICP profiles may contribute to the cellular injury reported after blast exposure. The goal of this study was to examine and identify the critical biomechanical contributions of the shock wave interactions using a rodent model of blast neurotrauma. Independent methods for measuring skull strain and ICP were applied. Subsequent analysis of the rodent skull was used to further characterize potential areas of skull flexure. Currently information regarding the response of the rat head to shock wave exposure is lacking in the literature and this series of experiments will provide much needed insights into the underlying biomechanics of blast neurotrauma.

METHODS

Wayne State University (WSU) Shock Wave Generator

The WSU shock wave generator is a shock tube system that is based on a commonly employed system for the generation of well formed, controlled shock waves.[9] The system has a driver section that is separated from the driven chamber by a frangible membrane and is pressurized with compressed helium. Upon membrane rupture, the rapid expansion of gas in the tube drives an air shock wave into the test section. The event is measured by pressure sensors (Model 102A06, PCB Piezotronics Inc.) at positions along the length of the shock tube. Shock wave amplitude is controlled by varying the thickness of the frangible membrane. As the thickness of the membrane increases, the pressure within the driver will increase prior to rupture of the diaphragm. The increased pressure during rupture of the diaphragm will generate greater shock wave amplitudes. Specific details of the WSU shock wave generator are documented in Leonardi *et al.*[14]

Animal Testing

Approval of all experiments was obtained from the Wayne State University Institutional Animal Care and Use Committee (IACUC) prior to testing. A total of ten male Sprague–Dawley rats, age 65–70 days old, were procured. All animals were given food and water *ad lib*. Animals were randomly assigned to one of two groups based on instrumentation used during the testing: strain gauge (SG) or ICP sensor mounted to the top of the skull (IC).

Animal Preparation and Sensor Installation for SG Testing

Five SG rats were sacrificed immediately prior to testing. The dermal tissue was removed from the medial dorsal surface of the head exposing a 1.5 cm wide region of the skull extending from 1 cm rostral to the bregma to 1 cm caudal to the lambda. The skull surface was then cleaned using acetone to ensure a solid and durable mechanical bond with the strain gauge. A 3-axis rectangular Rosette-style strain gauge (FAER-25B-35SX, Vishay Micro-measurements Inc.) was then attached to the skull surface using

cyanoacrylate and allowed five minutes to cure. To limit motion of the rat's head during exposure and prevent mechanical stress on the instrumentation wires, the nose was secured such that the head was pitched down at approximately 45° to the shock front. The channels were named rostral, medial, and caudal (Fig. 1a).

Animal Preparation and Sensor Installation for IC

Five IC designated rats were anesthetized using a ketamine/xylazine mixture (80 mg/kg/10 mg/kg; I.P.) and immobilized in a stereotaxic frame. A longitudinal incision was made along the dorsal medial surface of the head, exposing the skull from the bregma to the lambda. A 1.5 mm diameter hole was drilled using a stereotaxic high-speed drill at the following location: +3.0 (A-P (mm) from Bregma), −2.0 (M-L (mm)), and −1.0 (D-V (mm)), exposing the frontal cortex.

A plastic guide cannula (18 gauge; 1.2 mm, CMA Microdialysis Inc.) with a small pedestal was implanted through the hole and fixed to the skull using two small stainless steel screws inserted at 45° angles from the horizontal into the skull adjacent to the cannula. Cranioplastic cement was applied to fix the pedestal to the skull and was anchored by the screws. The surgical wound was closed with sutures, as needed. A dummy cannula insert with a threaded cap was inserted in the guide cannula until shock exposure; the rats were allowed five days recovery time.

Prior to testing, rats were anesthetized using a ketamine/xylazine mixture (80 mg/kg/10 mg/kg; I.P). The cannula was then filled with a sterile saline solution. The cannula cap was filled with petroleum jelly and the fiber optic pressure sensor (FOP-MIV, Fiso Inc.) was inserted into the cannula and threaded onto the cannula pedestal. Figure 1b provides a sketch of the technique applied.

Shock Wave Exposure

The rat was affixed to a trolley-mounted stage using a nylon harness, and inserted into the shock tube, such that its nose was positioned 114 cm inside the end of the Lexan® tube opposite to, and facing, the driver (Fig. 2). The harness maintained the rat's longitudinal axis perpendicular to the shock front and in fixed proximity to a side-on pressure sensor. The trolley system reduced the effects of post-shock dynamic pressure flow on the rat.

Once placed in the harness, the SG rats were subjected to three exposures each at 69, 97, 117, and 172 kPa static shock pressure or until sensor failure, thus a total of 12 exposures per animal. The IC rats were exposed to three repeated exposures at three intensities (69, 97, and 117 kPa). In order to conserve the integrity of the ICP sensors, the highest pressure

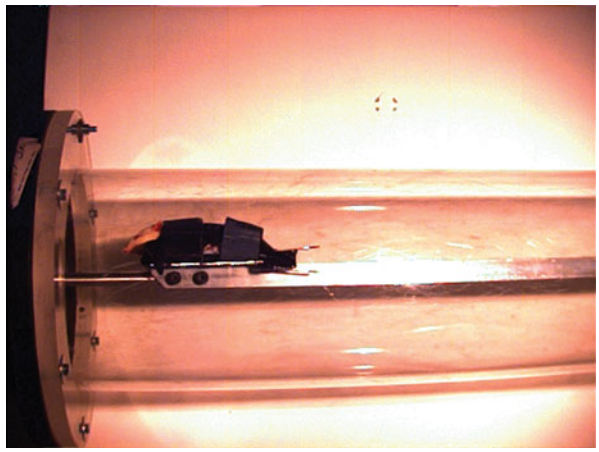

FIGURE 2. The rat was placed 114 cm within the shock tube and was placed on a trolley system to reduce the level of dynamic pressure shifts that are not representative of a free field shock wave.

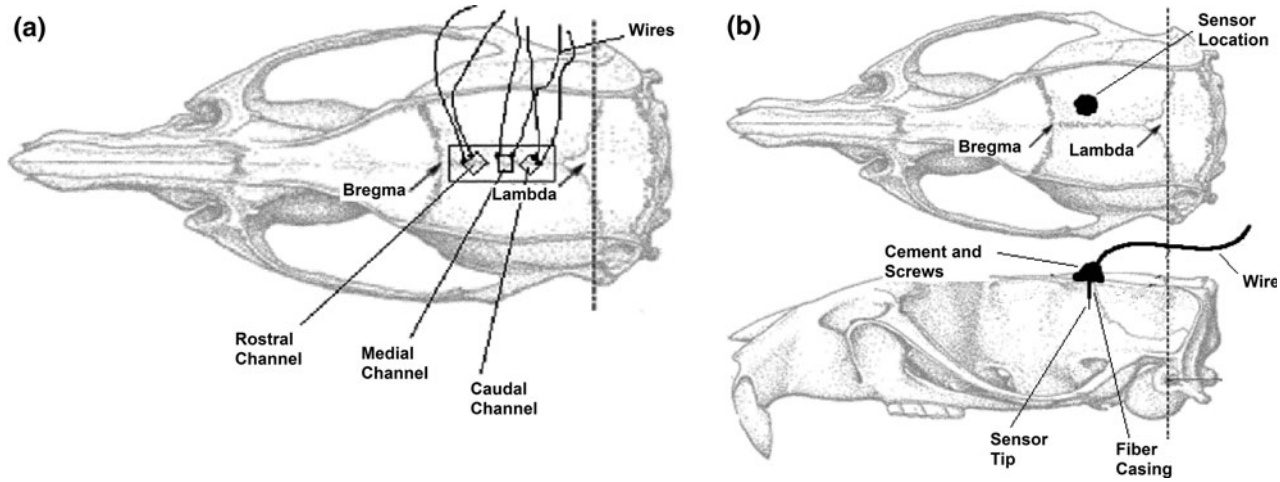

FIGURE 1. Placement of strain gauge on surface of the rat skull (a). Fiber optic pressure sensor installation on a rat skull (b).

intensity (172 kPa) was not applied. The intensities used in the protocol were determined from previous tests to maximize the amount of useful data. The time in between exposures was approximately two minutes for both groups of animals.

Both ICP and strain data were collected at 400 kHz using the Dash 8HF data acquisition system (Astromed Inc.). The data was then post-processed completely using Diadem 11.0 (National Instruments Inc.). Calculations of maximum principal strain were made using the formula below; the rostral channel was measured as ε_1, the medial channel was measured as ε_2, and the caudal channel was measured as ε_3.

$$\varepsilon_{P,Q} = \frac{\varepsilon_1 + \varepsilon_3}{2} \pm \sqrt{\left[(\varepsilon_1 - \varepsilon_2)^2 + (\varepsilon_2 - \varepsilon_3)^2\right] / 2}$$

The data was then reported in microstrain, and the magnitude of the first compressive peak was recorded. The IC pressure data was also analyzed, including peak pressure and rate of pressure change. Data was grouped by shock wave intensity and responses were compared using ANOVA with *post hoc* Tukey HSD used to determine significant differences ($p < 0.05$) between groups.

Computer Tomography (CT) Imaging

Following the experimental test series, computed tomography (CT) scans were obtained for the SG rats by means of a microCT device (Scanco VivaCT, Scanco Medical Inc.). ICP rats were not scanned as the instrumentation installed into the skull made it difficult to measure bone thickness. Variability of SG rat skull thickness throughout the skull was determined to help identify structural weaknesses that could be considered candidates for flexure. Skulls were scanned using a voltage of 70 kVp and current of 114 μA at a 30 μm resolution with a 320 ms integration time. Thickness measurements were calculated by using microCT analysis software (Scanco Medical Inc.). Measurements were taken at the midpoint between the lambda and bregma sutures. Three-dimensional reconstruction of the skull was undertaken to appreciate the skull geometry.

RESULTS

SG Measurements

The data collected from the strain gauges was useful for determining the flexural response of the superior braincase to shock wave loading. There were characteristic superimposed response patterns that were observed consistently as follows: (1) A strong and rapid compression with an associated damped oscillation at relatively high frequency (less than 3 kHz). (2) A quasi-steady decompression closely following the decay of the external static overpressure condition that developed as the strain returned to pre-blast levels. (3) A waveform of lower frequency with its pulse beginning in tension following the rapid compression. These responses were present for all the rats tested and are shown in Fig. 3.

The waveforms from two different rats are presented in Fig. 3, and the characteristic responses described prior are observable for both series. The first trace in each series is from the side-on (static) pressure sensor exposed to the incident shock wave. Within both series, following the incident shock, reflections from the fixture holding the specimen develop and create pressure artifacts on the sensor's surface that are not representative of the environment to which the specimen is exposed. This effect is expected from theory; the arrival and amplitude of the perturbation coincides with those expected of that reflection disturbance; confirmation of this phenomenon is also demonstrated by the fact that the shock reflections are similar between series, while the strain response is specific to the specimen being tested.

The peak compression was reported for all exposures. In Fig. 4a, it is shown that as the incident shock wave intensity increased, the calculated maximum principal strain also increased. The means were significantly different between groups ($^*p < 0.05$).

ICP Measurements

For the ICP profiles, two response patterns were observed consistently between specimens. (1) The peak compression wave will rebound and oscillate in a dampened harmonic motion. (2) There was a rapid increase in pressure that approximates the external loading environment and then returns to pre-exposure conditions. In Fig. 4b, 4c it is shown that as the incident shock wave intensity increased, the peak pressure and maximum rate of pressure change both increased.

The pressure response profiles for a 249 gm rat are shown in Fig. 5. The three profiles have been time shifted to begin at the same point. The increase in peak pressure as a function of an increase in incident side-on pressure can be observed for this series of wave forms. The duration of the rise times is also a function of intensity, where the greatest intensities resulted in the shortest rise times. To further this point, the 97 kPa ICP wave form was time shifted so that its pressure profile could be compared to a 97 kPa incident shock wave without the shock reflections that were observed in Fig. 5 (Fig. 6). The rise times between the incident wave as measured by the side-on pressure sensor and the ICP wave is of interest (27 compared to 195 μs). Although the rise time of the shock front is

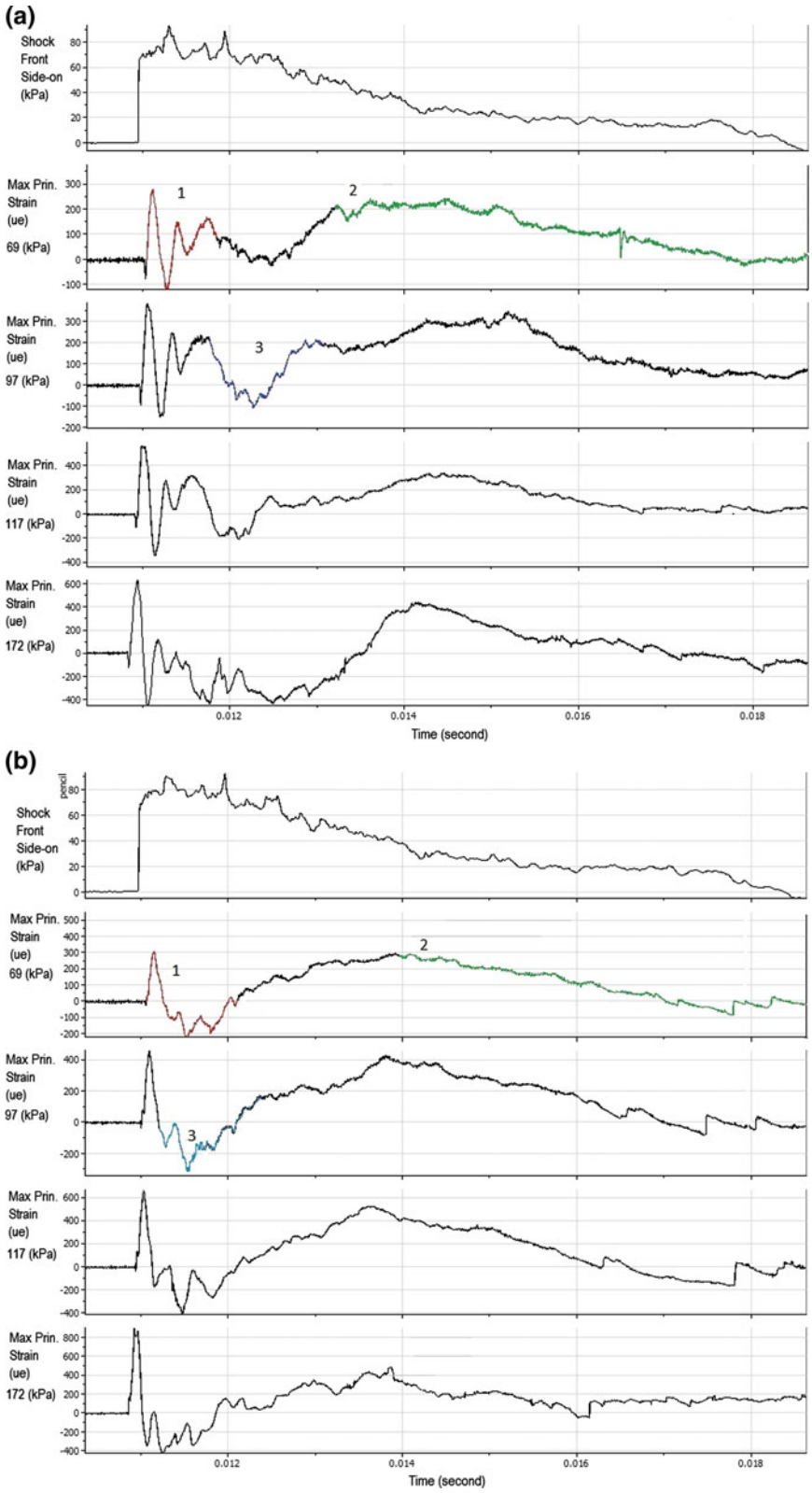

FIGURE 3. The principal strain response profiles of the superior brain case for both a 262 and 247 gm rat when exposed to shock waves of increasing intensity. The magnitude for each profile is adjusted so that the frequency content is observable. For the presented data, tension is negative and compression is positive. (1) A strong and rapid compression with an associated damped oscillation at relatively high frequency (less than 3 kHz). (2) A quasi-steady decompression closely following the decay of the external static overpressure condition that developed as the strain returned to pre-blast levels. (3) A waveform of lower frequency with its pulse beginning in tension following the rapid compression.

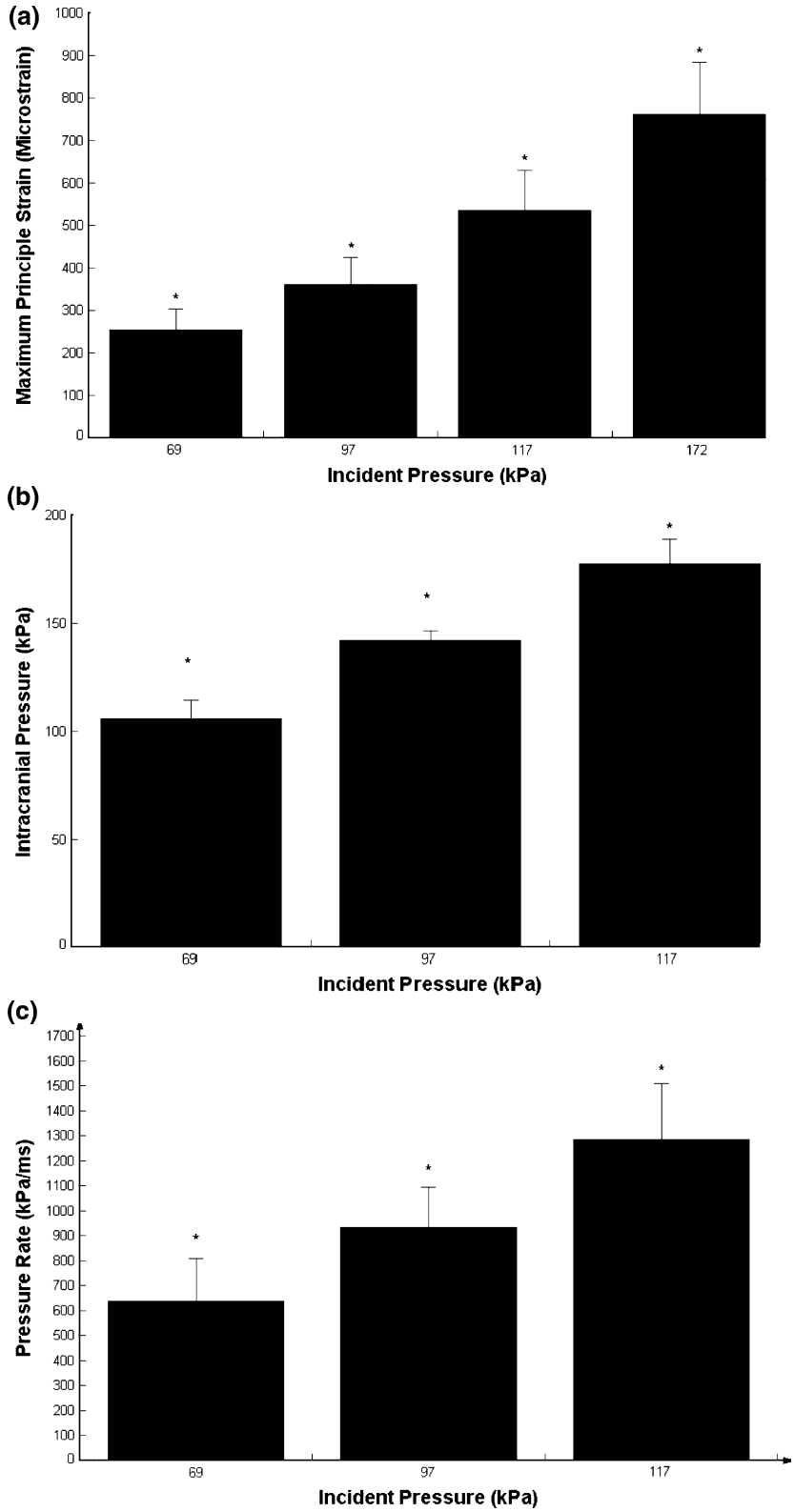

FIGURE 4. (a) The initial compression of the skull is dependent on intensity of the incoming shock wave. The largest magnitude shock waves caused the greatest maximum principal strains. All groups were significantly different from each other (*$p < 0.05$). (b) The ICP will increase beyond that of the incident shock wave (*$p < 0.05$). (c) The rate of pressure change will also increase with intensity (*$p < 0.05$).

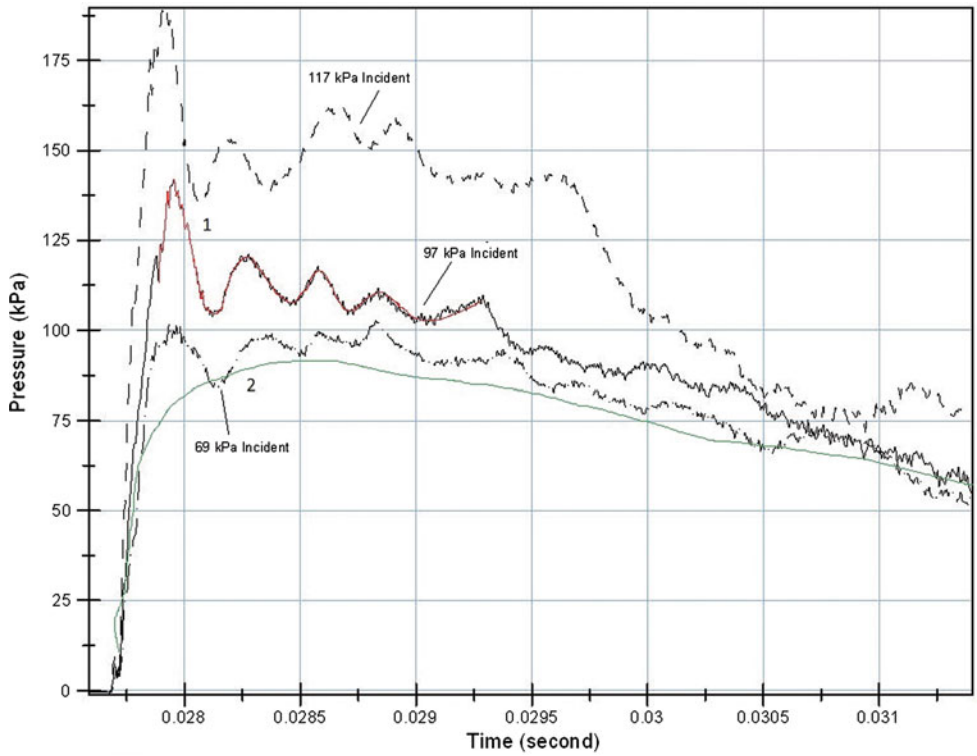

FIGURE 5. The intracranial pressure response of a rat skull is dependent on shock wave intensity. The ICP responses for a 249 gm rat show distinct pressure fluctuations (1) (red) that are present in each of the profiles that last for less than 2 ms. The waveforms will also approximate the external loading response invoked by the shock wave (2) (green).

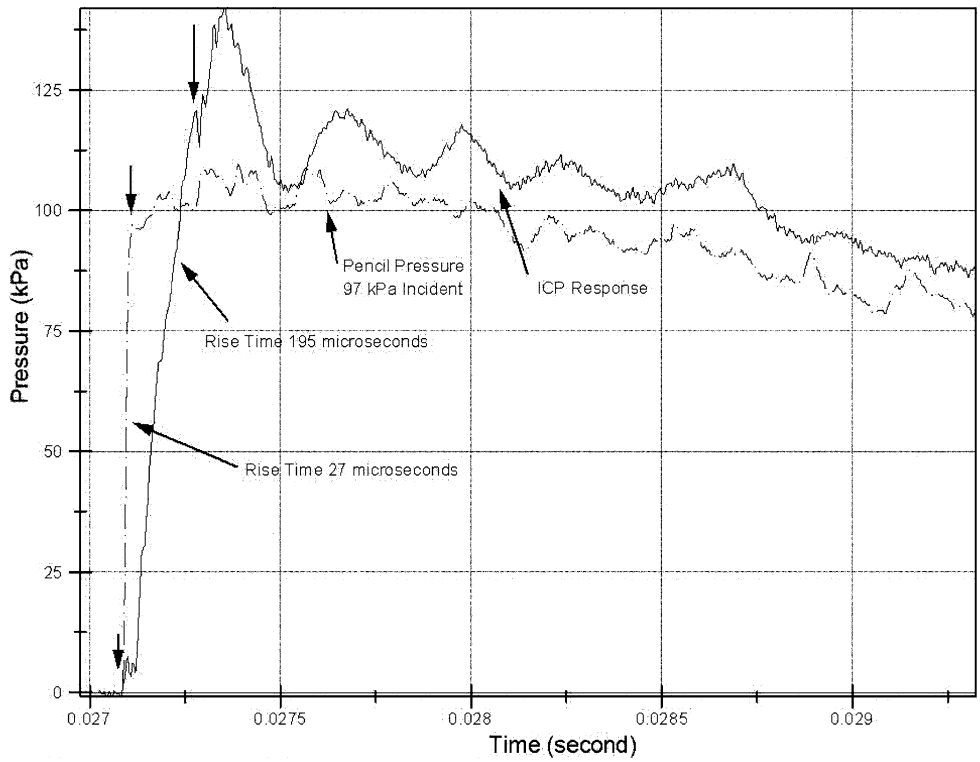

FIGURE 6. The rise time of the external pressure wave is faster than the rise time of the record intracranial pressure for a 249 gm rat. It is hypothesized that this is due to the amount of energy that is required to deform the skull so that a pressure wave can develop within the brain.

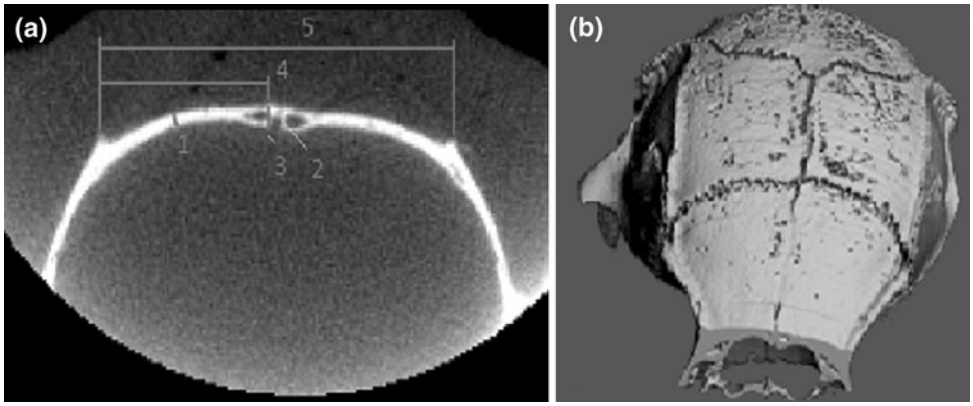

FIGURE 7. (a) Measurements were taken of the MicroCT images of the rat skull to determine key structural elements. (b) A three-dimensional reconstruction of the images depict that there are considerable gaps between the bone plates with significant reinforcement on the lateral bone folds, suggesting that the midline suture will be a probable place for skull flexure to take place.

approximately 1 μs the 27 μs measured is an artifact that is created by displacing the sensing element. It is expected that this delay between the two pressure profiles is caused by the absorption of energy that takes place by causing the skull to flex, thereby increasing ICP.

MicroCT Imaging

The results from the microCT imaging provided information regarding the geometry and thickness of specific bones in the skull (Fig. 7a). The mid-plate thickness between lambda and bregma sutures was approximately 0.354 ± 0.061 mm thick (1) where the thickness increases near the midline suture to 0.630 ± 0.082 mm thick (3). The gap between the suture itself was approximately 0.162 ± 0.016 mm thick (2). At this point the distance from horn to horn was 11.72 ± 0.114 mm (5). Additionally the distance from horn to suture top was 5.78 ± 0.207 (4). A sample of measurement locations are indicated in Fig. 7a. The image is of a cross section of head mid-distance between the lambda and bregma sutures. The term horn is in reference to the folds of bone on the lateral aspects of the skull, acting as reinforcements. Values are reported as (mean $\pm$ SD).

In Fig. 7b a three-dimensional reconstruction of the rat skull is provided. The rostral end was rotated down to the bottom of the graphic; the caudal region is near the top. The locations of the suture lines indicate that inward flexure of the superior bones of the skull case is probable during exposure due to the static pressure as it traverses the head.

DISCUSSION

Recent experimental biomechanical data for the rat suggested that skull flexure contributes to the ICP gradients developed within the brain as a result of shock wave interaction.[14] Results from the current experiments validate the hypothesis by Leonardi *et al.*[14] demonstrating that strain on the skull surface may have a significant effect on the imparted ICP waveform. By applying a series of pressure intensity exposures, it was observed in this study that the ICP response was dependent on the incident shockwave intensity. Further, the rate of pressure change was found to increase while the rise time to peak pressure was found to decrease with intensity.

When the ICP response was compared to the pressure profile of the incident shock wave, a delay in the rise time of the ICP was observed. This suggests that the rat skull is acting as a medium between the external environment and the intracranial contents. Pressure recordings reported by Bauman *et al.*[2] also found a significant delay in the rise time of the ICP profile compared to the incident shock wave during their swine testing. It is hypothesized that the rise time of those ICP profiles within the swine will be longer than that of the rat because of the difference in skull thickness between species. More studies need to be conducted to verify this relationship.

The microCT imaging of the superior braincase of the rat revealed that the bones are not completely fused and the lateral aspects are reinforced with thicker layers of bone. It is hypothesized that when the incident shock wave traverses the surface of the skull, the shock wave is acting as a moving load. This loading will cause the greatest deflections in the regions with the least reinforcement. When examining the specific anatomical features of the rat skull, the region between the lambda and bregma suture appears to offer the greatest amount of deflection as the bone plates may hinge about the major sutures.

The results from the strain gauge data further substantiates the hypothesis that the incident shock wave

is causing the skull to flex. The rapid compression that increases in magnitude with the intensity of the incident shock is believed to be the direct result of the shock wave compressing the skull surface. The damped harmonic oscillation phase that then developed as a result of the compression is hypothesized to be due to the return of the deflected surface regions back to equilibrium. The quasi-steady decompression phase that approximates the external pressure environment is then best observed due to the dispersion of the energy from the rapid compression of the skull case. The nature of the secondary surface wave beginning in tension has yet to be determined. It has been observed that this wave is dependent on the intensity of the incident shock wave. The front of this wave will be steeper as the intensity increases. Research is ongoing to determine the nature of this wave.

Because of these observations in both the strain gauge and ICP responses, it is proposed that there are two major regions in the waveform response. The first is the transient phase which consists of a rapid compression and harmonic oscillations; the other is the quasi-steady decompression phase. It is possible that the most damaging aspect of these waveforms is the initial oscillations that may cause high levels of strain rates in both tension and compression that could be transferred as rapid compression waves within the brain due to the coupling at the skull/dura interface.

Some limitations exist with the current data. The placement of the strain gauge on the skull is problematic because mounting on the suture lines will cause an amplification of the signal. Although the results provided key information, the principal strain calculations were not made on a homogenous surface and the sensors were relatively widely distributed. But, given the consistency of the signals between exposures and that similar responses were observed between species, the data is useful for describing responses of the rat skull to shock wave exposure.

The ICP data was of concern because the skull was modified with small screws and bone cement, modifying the native surface. If the superior skull case is acting as a diaphragm, the additional mass of the sensor cement complex will cause the periodic oscillations to have a response with fewer competing frequencies than what are observed in the strain profiles. This can be seen in Fig. 5, specifically for the 97 kPa incident exposure. Additionally, it still needs to be determined to what extent the fiber optic sensors are mapping the motion of the skull when compared to the environment within the brain. Because of the artifacts of testing with the ICP sensors, direct relationships were not made to the strain gauges. Further studies are required to address this issue.

It is expected that the biomechanical responses of the rat will be unique when compared to other species. It would be ideal to be able to equate injury responses in rats to humans, but scaling for thresholds of injury cannot be conducted until the mechanism of injury is discovered. The human head is much more spherical and thicker in geometry as compared to the rat. These changes may result in different response modes than what are observed in the rat. Because the mechanical inputs into the brain are likely specific to the system, a multi species analysis of skull flexure and ICP will need to be undertaken.

In summary, this article provides key biomechanical data which suggests that skull flexure may be one of the major factors for causing ICP gradients. The superior rat skull is a location where flexure will be exaggerated. Since neuronal injury is dependent on strain rate, it is hypothesized that the first two ms following exposure (the transient phase) is the likely timeframe for causing neurotrauma. This period is composed of extremely rapid shifts in strain that are likely transmitted to the cells within the brain. It is not yet known which aspects of the intracranial pressure profile causes cellular injury. Ultimately, it is of utmost importance to evaluate cellular vulnerability under the particular stress-rate conditions observed. Utilizing appropriate *in vitro* experiments for blast-related neurotrauma will help identify biomarkers of neuropathology and shifts in gene expression occurring as a result of shock wave exposure.

ACKNOWLEDGMENTS

We would like to thank the WSU Bioengineering Center staff and students for assisting with this project. We would also like thank Dr. Amanda Esquivel for obtaining the CT images. This project was partially funded by DOD Award Number W81XWH-08-2-0207 and the Thomas J. Rumble Fellowship.

REFERENCES

[1]Battacharjee, Y. Shell shock revisited: solving the puzzle of blast trauma. *Science* 319:406–408, 2008.

[2]Bauman, R., G. Ling, L. Tong, A. Januszkiewicz, D. Agoston, N. Delanerolle, J. Kim, D. Ritzel, R. Bell, J. Ecklund, R. Armonda, F. Bandak, and S. Parks. An introductory characterization of combat casualty care relevant swine model of closed head injury resulting from exposure to explosive blast. *J. Neurotrauma* 26:841–876, 2009.

[3]Cernak, I. Penetrating and blast injury. *Restor. Neurol. Neurosci.* 23:139–143, 2005.

[4]Chafi, M., G. Karami, and M. Ziejewski. Biomechanical assessment of brain dynamic responses due to blast pressure waves. *Ann. Biomed. Eng.* 38:490–504, 2010.
[5]Chavko, M., W. Koller, W. Prusaczyk, and R. McCarron. Measurement of blast wave by a miniature fiber optic pressure transducer in the rat brain. *J. Neurosci. Methods* 159:277–281, 2007.
[6]Clemedson, C., and C. Criborn. Mechanical response of different parts of a living body to a high explosive shock wave impact. *Am. J. Physiol.* 181:471–476, 1955.
[7]Courtney, M., and A. Courtney. Working toward exposure thresholds for blast-induced traumatic brain injury: thoracic and acceleration mechanisms. *Neuroimage* 54:S55–S61, 2011.
[8]Finkel, M. The neurological consequences of explosives. *J. Neurol. Sci.* 249:63–67, 2006.
[9]Henshall, B. Shock tube–versatile tool of aerodynamic research. *J. Royal Aeronaut. Soc.* 58:541–546, 1954.
[10]Hicks, R., S. Fertig, R. Desrocher, W. Koroshetz, and J. Pancrazio. Neurological effects of blast injury. *J. Trauma* 68:1257–1263, 2010.
[11]Hoge, C., D. McGurk, J. Thomas, A. Cox, C. Engel, and C. Castro. Mild traumatic brain injury in U.S. Soldiers returning from Iraq. *N. Engl. J. Med.* 358:453–463, 2008.
[12]Kluger, Y., A. Nimrod, P. Biderman, A. Mayo, and P. Sorkin. The quinary pattern of blast injury. *Am. J. Disaster Med.* 2:21–25, 2007.
[13]Lechner, R., G. Achatz, T. Hauer, H. Palm, A. Lieber, and C. Willy. Patterns and causes of injuries in a contemporary combat environment. *Unfallchirurg* 113:106–113, 2010.
[14]Leonardi, A., C. Bir, D. Ritzel, and P. VandeVord. Intracranial pressure increases during exposure to a shock wave. *J. Neurotrauma* 28:85–94, 2011.
[15]Ling, G., and J. Ecklund. Traumatic brain injury in modern war. *Curr. Opin. Anaesthesiol.* 24:124–130, 2011.
[16]Luks, F. Blast injuries—and the pivotal role of trauma surgeons. *Acta Chir. Belg.* 110:517–520, 2010.
[17]Moss, W., M. King, and E. Blackman. Skull flexure from blast waves: a mechanism for brain injury with implications for helmet design. *Phys. Rev. Lett.* 103:108702, 2009.
[18]Mott, F. On the effects of high explosives upon the central nervous system. *Lancet* 187:331–338, 1916.
[19]Risling, M. Blast induced brain injuries—a grand challenge in TBI research. *Front. Neurol.* 8:1, 2010.
[20]Romba, J., and P. Martin. The propagation of air shock waves on a biophysical model. US Army Ordinance Technical Memorandum, pp. 17–61, 1961.
[21]Stuhmiller, J., K. Ho, M. VanderVorst, K. Dodd, T. Fitzpatrick, and M. Mayorga. A model of blast overpressure injury to the lung. *J. Biomech.* 29:227–234, 1996.
[22]Taylor, P., and C. Ford. Simulation of blast-induced early time intracranial wave physics leading to traumatic brain injury. *J. Biomech. Eng.* 131:061007, 2009.